M.Tech (Geoinformatics) **Gaurav Singh** **2023**

ASSESSMENT OF RIVER WATER QUALITY PARAMETERS USING SATELLITE DATA

A DISSERTATION

SUBMITTED IN PARTIAL FULFILMENT OF THE REQUIREMENTS

FOR THE AWARD OF THE DEGREE

OF

MASTER OF TECHNOLOGY

IN

CIVIL ENGINEERING

(With Specialization in Geoinformatics Engineering)

Submitted By:

GAURAV SINGH

(2K21/GEO/05)

Under the supervision of

DR. (COL) K.C. TIWARI, PROFESSOR

MULTIDISCIPLINARY CENTRE FOR GEOINFORMATICS

DEPARTMENT OF CIVIL ENGINEERING

DELHI TECHNOLOGICAL UNIVERSITY

(Formerly Delhi College of Engineering)

Bawana Road, Delhi – 110042

MAY 2023

ASSESSMENT OF RIVER WATER QUALITY PARAMETERS USING SATELLITE DATA

A DISSERTATION

SUBMITTED IN PARTIAL FULFILMENT OF THE REQUIREMENTS
FOR THE AWARD OF THE DEGREE
OF

MASTER OF TECHNOLOGY
IN

CIVIL ENGINEERING
(With Specialization in Geoinformatics Engineering)

Submitted By:

GAURAV SINGH
(2K21/GEO/05)

Under the supervision of

DR. (COL.) KAILASH CHANDRA TIWARI, PROFESSOR

MULTIDISCIPLINARY CENTRE FOR GEOINFORMATICS
DEPARTMENT OF CIVIL ENGINEERING
DELHI TECHNOLOGICAL UNIVERSITY
(Formerly Delhi College of Engineering)
Bawana Road, Delhi – 110042

MAY 2023

CANDIDATE'S DECLARATION

I, Gaurav Singh, Roll No. 2K21/GEO/05 student of M. Tech (Geoinformatics), hereby declare that the Dissertation titled "Assessment of River Water Quality Parameters Using Satellite Data" which is submitted by me to the Multidisciplinary Centre for Geoinformatics, Department of Civil Engineering, Delhi Technological University, Delhi in partial fulfillment of the requirement for the award of the degree of Master of Technology, is original and not copied from any source without proper citation. This work has not previously formed the basis for the award of any Degree, Diploma Associateship, Fellowship, or other similar title or recognition.

Place: Delhi GAURAV SINGH

Date: May 31, 2023

CERTIFICATE

I hereby certify that the Project Dissertation titled, "Assessment of River Water Quality Parameters Using Satellite Data" which is submitted by me to the Multidisciplinary Centre for Geoinformatics, Department of Civil Engineering, Delhi Technological University, Delhi in partial fulfillment of the requirement for the award of the degree of Master of Technology, is a record of the project work carried out by the student under my supervision. To the best of my knowledge, this work has not been submitted in part or full for any Degree or Diploma to this University or elsewhere.

Place: Delhi

Date:

Dr. (Col) K.C TIWARI
SUPERVISOR
Professor,
Multidisciplinary Centre for Geoinformatics
Department of Civil Engineering
Delhi Technological University
(Formerly Delhi College of Engineering)
Bawana Road, Delhi – 110042

ABSTRACT

The assessment of the river quality is a tedious task and takes a long time to calculate the river quality via the traditional methods. There is a chance of inaccuracy in the results due to several factors. With the use of satellite imaging methods, we can conveniently monitor and assess the river water quality and can easily cover the whole river in a single day. This study was made to calculate different water quality parameters in the Yamuna River.

27 different locations starting from Hathnikund Barrage to Hathi Ghat were covered. The parameters such as land surface temperature, pH, salinity, turbidity, chlorophyll, suspended matters, dissolved oxygen (DO), dissolved organic matter (DOM), etc were calculated using different satellite data and integrated with the ground-based data using the ArcGIS.

Considering the Landsat satellite data to process the visualization of the area using the False Colour (Vegetative Analysis) and the Natural Colour composite using the combination of 6,5,4 and 4,3,2 respectively. The Sentinel-2 satellite data is also considered for visualization of the area using the False Colour and the Natural Colour composite using the combination of 8,4,3 and 4,3,2 respectively and the calculation of some specific parameters' formulas using the raster calculator in the ArcGIS software.

The integration of satellite and ground-based data using ArcGIS provides a comprehensive understanding of water quality parameters and helps identify areas that require attention for water quality management. The study emphasizes the importance of collaboration and data sharing among researchers to promote the development of more robust models for estimating water quality parameters.

ACKNOWLEDGEMENT

First and foremost, I express my heartfelt gratitude to the Almighty God for providing me with strength, sustenance, and blessings throughout my academic journey, leading up to the completion of this master's thesis. It is through His grace that I have achieved success in all my academic pursuits thus far.

I extend my sincere appreciation and gratitude to my impeccable and ever-supportive supervisor, Dr. (Col) K. C. Tiwari, for his invaluable guidance and empathetic approach throughout my research. His cooperation, appreciation, constructive criticism, and motivation have been instrumental in helping me overcome various challenges and obstacles along the way.

I would like to acknowledge the significant contribution of Atulya Ganga in my M. Tech thesis. Their expertise, insights, and support have greatly enriched the content and findings of this research work. Their involvement has been instrumental in ensuring the quality and depth of this thesis.

I am deeply indebted to the unwavering support of all the members of The Multidisciplinary Centre for Geoinformatics, Delhi Technological University, who have always been available whenever I needed assistance. I also want to recognize and appreciate the invaluable assistance I received from my fellow batch mates throughout these months of research.

I would like to express my heartfelt thanks to all my near and dear ones, including my family, relatives, and friends, for their unwavering support, understanding, and encouragement that kept me motivated throughout this journey. Lastly, I want to express my gratitude to everyone who stood beside me during this journey, playing a part in keeping me focused and motivated.

Gaurav Singh

Contents

CANDIDATE'S DECLARATION iii

ABSTRACT v

ACKNOWLEDGEMENT vi

LIST OF FIGURES ix

LIST OF TABLES xi

LIST OF ABBREVIATIONS xii

CHAPTER 1 1

INTRODUCTION 1

1.1 MOTIVATION 1

1.2 PROBLEM STATEMENT 2

1.3 LITERATURE REVIEW 3

1.4 RESEARCH GAPS 5

1.5 OBJECTIVES 6

1.6 THESIS OVERVIEW 6

CHAPTER 2 7

DETAILED REVIEW OF VARIOUS WATER QUALITY PARAMETERS, EXTRACTION OF THESE PARAMETERS USING LAB EXPERIMENTS 7

2.1 WATER QUALITY 7

2.2 WATER QUALITY PARAMETERS 7

2.3 SELECTION OF WATER QUALITY PARAMETERS 8

2.4 LIMITATIONS 11

CHAPTER 3 12

DETAILED REVIEW OF EXISTING LITERATURE ON EXTRACTION OF WATER QUALITY PARAMETERS USING SATELLITE DATA 12

3.1 OVERVIEW 12

3.2 WORKS RELATED TO SATELLITE DATA IN WATER QUALITY 13

3.3 APPLICATIONS, CHALLENGES, AND LIMITATIONS 16

3.3.1 Applications 16

3.3.2 Challenges 16

3.3.3 Limitations 17

CHAPTER 4............... 18

TO ASSESS A RELATIONSHIP BETWEEN THE GROUND-BASED DATA AND THE DN VALUE AVAILABLE FROM SATELLITE DATA FOR YAMUNA RIVER 18

4.1 OVERVIEW 18

4.2 STUDY AREA 18

4.3 DATA USED 22

4.4 METHODOLOGY 26

4.5 RESULTS 28

4.6 CONCLUSION 47

REFERENCES............... 48

LIST OF FIGURES

Figure 3.1 A Diagram on Applications of Remote Sensing for Water ………….……….12

Figure 4.1 Study Area Map…………………………….…………………………21

Figure 4.2 Landsat tiles opened in ArcMap along with the boundaries and river shapefile…..23

Figure 4.3 NDWI Methodology….…………………………………….……...23

Figure 4.4 NDWI Map……….…………………………………….………...24

Figure 4.5 Online Maps Portal………………………………….…….…...25

Figure 4.6 General Methodology Applied for Maps Generation ……………………………27

Figure 4.7 Model Generated Map…………………………...……………………………28

Figure 4.8 Generated pH Graph…………...…………………………………...……29

Figure 4.9 pH (in-situ) vs pH (sat)…………………. ………...…………………………...29

Figure 4.10 Salinity Map...……………...………………...……………………………31

Figure 4.11 Salinity Graph……………...………………...……………………………31

Figure 4.12 Turbidity Map………...……...………………...…………………….……33

Figure 4.13 Turbidity Graph……………...…………………...……………………………33

Figure 4.14 Turbidity (in-situ) vs Turbidity (sat)……………………...……………………34

Figure 4.15 Land Surface Temperature Methodology………....……………………………35

Figure 4.16 Land Surface Temperature Map………………...……………………………37

Figure 4.17 Land Surface Temperature Graph………………...…………………………..37

Figure 4.18 Temperature (in-situ) vs Temperature Calculated..……………………………..38

Figure 4.19 Chlorophyll Map……………...………………...……………………………39

Figure 4.20 Chlorophyll Graph……………...……………...……………………………40

Figure 4.21 Total Dissolved Solids Map….…………………...……………………………….41

Figure 4.22 Total Dissolved Solids Graph...…………………...……………………………….41

Figure 4.23 TDS (in-situ) vs TDS (sat)……………....………...……………………………….42

Figure 4.24 Coloured Dissolved Organic Matter Map.………...……………………………….43

Figure 4.25 Coloured Dissolved Organic Matter Graph…...…...……………………………….43

Figure 4.26 Dissolved Oxygen Map………….………………...……………………………….45

Figure 4.27 Dissolved Oxygen Graph.........…………………...……………………………….45

Figure 4.28 DO (in-situ) vs DO (sat).........…………...……….....……………………………….46

LIST OF TABLES

Table 2.1 Different Parameters ……………………..……………….…………………………………...7

Table 4.1 Reference of Locations………………………………………………………………….19

Table 4.2 Reference of Ground Truth for Validation….…………………….……………….20

Table 4.3 Reference of Landsat Satellite Images……………………………………………….22

Table 4.4 Reference of Sentinel-2 Satellite Images……………………………………………..22

Table 4.5 Algorithms Used for Model Builder………………………………………………….26

Table 4.6 Range of NDSI Classes…………………………………………………………………30

Table 4.7 Range of Turbidity in NTU……………………………………...……………….32

Table 4.8 Range of Total Dissolved Solids……………………………………………….……..40

Table 4.9 Range of Coloured Dissolved Organic Matter in mg/L^{-1} …………………….……….42

Table 4.10 Range of Dissolved Oxygen in p.p.m…………………………...………………...44

LIST OF ABBREVIATIONS

APHA	American Public Health Association
AWWA	American Water Works Association
ANN	Artificial Neural Network
ASTER	Advanced Spaceborne Thermal Emission Reflection Radiometer
BOD	Biochemical Oxygen Demand
BIS	Bureau of Indian Standards
BT	Brightness Temperature
CDOM	Coloured Dissolved Organic Matter
COD	Chemical Oxygen Demand
Chl-a	Chlorophyll
CPCB	Central Pollution Control Board
DS	Dissolved Solids
DO	Dissolved Oxygen
DN	Digital Number
EC	Electrical Conductivity
ETM	Enhanced Thematic Mapper
ETM+	Enhanced Thematic Mapper Plus
EOS	Earth Observation Satellite
GIS	Geographical Information System
IRS	Indian Remote Sensing
IS	Indian Standard

KML	Keyhole Markup Language
LST	Land Surface Temperature
MERIS	Medium Resolution Imaging Spectrometer
MSI	Multispectral Instrument
NDTI	Normalize Difference Turbidity Index
NTU	Nephelometric Turbidity Units
NDWI	Normalised Difference Water Index
NIR	Near-Infrared
NIC	National Informatics Centre
NDSI	Normalized Difference Soil Index
NDVI	Normalized Difference Vegetation Index
OLI	Operational Land Imager
OLCI	Ocean and Land Colour Instrument
OIP	Overall Pollution Index
PPT	Parts Per Thousand
WHO	World Health Organisation
WQI	Water Quality Index
RS	Remote Sensing
SDD	Secchi Disk Depth
SWI	Short Wave Infra-Red
SS	Suspended Solids
TN	Total Nitrogen
TP	Total Phosphorous

TM	Thematic Mapper
TSM	Total Suspended Material
TH	Total Hardness
TS	Total Solids
TDS	Total Dissolved Solids
TSS	Total Suspended Solids
TOC	Total Organic Carbon
TIRS	Thermal Infrared Sensor
TOA	Top of Atmospheric
VNIR	Visible-Near Infrared (VNIR)
WPCF	Water Pollution Control Federation

CHAPTER 1

INTRODUCTION

1.1 MOTIVATION

The motivation for conducting research on the assessment of river water quality parameters using satellite data lies in the potential to move forward with a new, advanced, cost-effective, and efficient solution for continuous monitoring and detection of pollution sources, identify spatial and temporal trends in water quality, and evaluate the health of rivers. Traditional methods of water quality assessment rely on in-situ measurements, which are often limited in spatial coverage, costly, and time-consuming. The recent advancements in satellite remote sensing present a unique opportunity to overcome these limitations, revolutionize the field of water quality assessment, and contribute to the sustainable management of water resources. By utilizing satellite imagery and advanced remote sensing techniques, we can obtain comprehensive and frequent information on key water quality indicators, such as turbidity, chlorophyll-a concentration, and temperature, over large-scale river bodies. The integration of satellite-derived water quality data with existing monitoring networks and models can lead to more accurate predictions and early warning systems for potential water quality issues.

1.2 PROBLEM STATEMENT

Water quality monitoring done via the in-situ measurement which is a time consuming and tedious process often leads to disadvantage of the emerging water quality problems like in obtaining or collecting the necessary information about water salinity, dissolved organic matter, coloured dissolved organic matter, dissolved oxygen, algal bloom detection. Poor water quality poses serious health risks to humans and animals that encounter contaminated water.

Monitoring water quality measures are essential for locating causes of pollution and implementing solutions. Traditional methods of monitoring can often be pricy, time-consuming, and restricted to a particular place. Therefore, methods for monitoring water quality parameters over wider areas must be implemented that are both cost-effective and economical.

Satellite imagery is an alternative method for monitoring water quality. Recent advancements in satellite technology have enable the detection of water quality parameters from space, offering an alternative to ground-based monitoring methods. The use of satellite data can provide wider coverage of water bodies, real-time monitoring, and cost savings compared to traditional methods. However, satellite data also have limitations, such as the need for accurate calibration and validation, atmospheric and cloud interference, and limited spatial resolution. This study explores Landsat 8/9 and Sentinel 2 satellite imagery for water quality monitoring.

Water quality monitoring is essential for protecting public health, ensuring sustainable use of resources, and mitigating negative impacts of human activities on aquatic ecosystems. However, traditional methods of water quality monitoring can be limited in their scope and accuracy, particularly in large or inaccessible water bodies. The use of satellite data has the potential to provide a more comprehensive and cost-effective approach to water quality monitoring. Despite the potential advantages, there are drawbacks to using satellite data. These drawbacks include the requirement for precise ground-truth data, restrictions on satellite data resolution, and difficulties in interpreting the data. Therefore, the problem statement is to assess the accuracy and reliability of using satellite data for monitoring river water quality parameters and to develop strategies for addressing the challenges associated with the approach.

1.3 LITERATURE REVIEW

Different methods either using in-situ measurements, remote sensing using models, spectral indexes, using ML approaches have been used to find different parameters which provide accurate results but validation via the in-situ measurement has been a factor to consider in many studies.

Abhishek Kumar Chaurasia, et al. (2018) [1] in the Varanasi district used the weighted arithmetic index method to determine the groundwater quality and the results showed that ~20% area ground water was non-suitable for drinking water as per the WQI classification.

A. K. M. Azad Hossain, et al. (2021) [2] used Landsat 8 OLI satellite imagery for determining the turbidity in the Tennessee River, U.S.A. They constructed a numerical turbidity estimation model by using the satellite photography and in-situ measurements.

Mohammad Haji Gholizadeh, et al. (2016) [3] suggested that different satellite sensors can be used for monitoring water quality parameters in various water bodies and concluded that remote sensing and GIS approaches combined with conventional in-situ sampling were the most efficient, least expensive, and most dependable technologies.

Min Wu, et al. (2009) [4] employed MODIS satellite data to monitor various water quality parameters such as Chl-a, SDD, TN, and TP. The findings of their study revealed that a straightforward, effective, and satisfactory model could be developed using multivariate regression analysis. However, it was noted that the precision of the model was relatively low.

Blake A. Schaeffer, et al. (2013) [5] reviewed different satellites like Sentinel-3, MODIS, MERIS, etc. and suggested that the emerging satellite technologies have the potential over traditional field sampling.

J. B. Alam, et al. (2007) [6] calculated water quality using the standard methods. Various water quality parameters such as APHA, AWWA, WPCF, etc. were discussed as part of the analytical approach. The results showcased that there were incidents where it was found that the water was certainly unfit for drinking purposes, that too without any form of treatment. High level of turbidity was identified in the water quality of the river stream during the monsoon season. Contrarily, higher concentration of BOD as well as faecal coliform was found during the dry season.

Osvaldo J. R. Pereira, et al. (2020) [7] estimated the ph using the Landsat 5 TM, Landsat 7 ETM+, and Landsat 8 OLI in the Nhecolândia Lakes (Brazilian Pantanal). For time-series data from 2002 to 2017, the model accurately predicted pH values using Landsat and synthetic bands, with an R^2 correlation of more than 85%.

Xiaoyan Wang & Wu Yang (2019) [8] did a systematic review on Water quality monitoring and evaluation using remote sensing techniques in China and suggested applications towards the sea areas than inland water resources as China have made commendable progresses in the water quality monitoring and evaluating using the remote sensing techniques, especially in inland lake.

D. Doxaran N, et al. (2004) [9] in the Tamar estuary (south-west UK) used the in-situ Hyperspectral Remote-Sensing Reflectance (Rrs) measurements to calculate TSM and CDOM. This resulted in obtaining linear relationships alongside a high correlation between the Rrs (850 nm)/Rrs (550 nm) ratio. Total suspended matter concentration and inorganic suspended matter concentration were discussed.

K.P. Sudheer, et al (2006) [10] used Landsat TM data with ANN model to calculate the suspended sediments and Chl-a. in the Beaver Reservoir in Northwest Arkansas. The study suggested that using derivative indices as input to develop ANN models was not an appropriate approach, as the performance of models developed based on the indices did not show good performance. Due to limitations of linear regression methods, applying ANN approach could significantly reduce the effort and computational time.

Shivangi Somvanshi, et al (2011) [11] estimated turbidity using NDTI and classify into low, moderate, and high classes of water turbidity for Gomti river of Lucknow using the Google Earth’s Quick-bird satellite imagery.

Somvanshi.S, et al. (2012) [12] used the IRS LISS III satellite for water analysis of TH, SS, DS, TS, pH, DO, Cl^-, BOD, COD and TH. The acceptable results were obtained considered for multiple linear regression analysis through 9 Variables except SS.

1.4 RESEARCH GAPS

The reviewed studies mainly focus on a relatively smaller part of the areas majorly the lakes and generally do not cover any state entirely. Also, these studies usually focus on the district as the smallest individual unit while neglecting the variation at even smaller administrative units. The parameters used are not consistent with all the studies as major researchers were considered either using 8 or 10 parameters.

The availability of satellite data is limited, particularly in developing countries. This can make it challenging to monitor water quality parameters consistently and across large geographic areas. The accuracy of satellite-derived water quality parameters needs to be validated with ground-based measurements. However, ground-based measurements are often limited, particularly in remote areas, making it challenging to validate the satellite data. A lack of standardization in the collection and processing of satellite data can lead to variations in the data, making it difficult to compare and analyse the results. There is a need to develop better models that can accurately estimate water quality parameters from satellite data. However, these models can be complex and may contain uncertainties, which can affect the accuracy of the estimates. The temporal coverage of satellite data can be limited due to cloud cover and other atmospheric conditions. This can make it challenging to capture the temporal variability of water quality parameters accurately.

According to the machine learning method used to evaluate the parameters affecting water quality using various methodologies, such as multivariate regression analysis, linear regression is the most straightforward but least accurate method. Multivariate regression offers a little boost to precision, but the use of neural networks can significantly increase retrieval performance. Most studies on machine learning for water quality prediction have focused on a single region or water body, making it difficult to assess the transferability of the models to other regions. Although machine learning algorithms have shown promise in improving water quality monitoring, there is limited research on how these algorithms can be integrated with traditional water quality monitoring methods to improve their accuracy and reliability.

1.5 OBJECTIVES

Considering the research gaps, this work has been based on the following objectives.

Objective 1. Detailed Review of Various Water Quality Parameters, Extraction of these Parameters Using Lab Experiments.

Objective 2. Detailed Review of Existing Literature on Extraction of Water Quality Parameters Using Satellite Data

Objective 3. To Assess a Relationship between the Ground-based Data and the DN Value Available from Satellite Data for Yamuna River.

Objective 4. To obtain a Water Quality Index Map.

1.6 THESIS OVERVIEW

This manuscript provides an introduction of the subject field in Chapter 2, then goes on to detail the resources used and the methods followed in Chapter 3, then goes to apply different approaches and validated the obtained result in Chapter 4 and conclude the notes on the study's effort as well as its findings.

CHAPTER 2

DETAILED REVIEW OF VARIOUS WATER QUALITY PARAMETERS, EXTRACTION OF THESE PARAMETERS USING LAB EXPERIMENTS

2.1 WATER QUALITY

Water quality is "the physical, chemical, and biological characteristics of water. Safe drinking water quality criteria were set forth by the Bureau of Indian Standards (BIS) (IS 10500:2012) [13]. In the absence of a different source, this standard provides the acceptable limits and the permissible limits. If any parameter such as a chemical or biological exceeds the allowable limit, a proper investigation ought to be carried out, and, if required, corrective measures ought to be carried out, or the use of the water supply for drinking needs to cease until the water quality is considered acceptable.

2.2 WATER QUALITY PARAMETERS

The parameters are broadly divided into three types namely physical, chemical, and biological but nowadays some parameters are further divided into heavy metals, pesticides, radioactive materials, etc.

Table 2.1: Different Parameters

Physical Parameters	Taste, Colour, Odour, Turbidity, pH, Temperature
Chemical Parameters	Silica, Potassium, Boron, Calcium (as Ca), Magnesium (as Mg), Total Hardness, Sulphide, Chloramines (as Cl_2), TDS/Elect. Conductivity, Total Alkalinity, Chloride, Fluoride, Ammonia, Nitrate, Nitrite, Sulphate,
Biological Parameters	Viruses (V. cholera, S. typhi, S. dysentrae, F. streptococci, Staphiloccocus, G. lamblia), Total coliform bacteria, E. coli/ Thermotolerant coliform bacteria
Heavy Metals	Mercury, Barium, Zinc, Aluminium, Selenium, Silver, Molybdenum (as Mo), Iron, Manganese, Copper, Total Chromium (as Cr), Cadmium, Lead, Nickel, Total Arsenic (as As),

Table 2.1: Different Parameters (Continued)

Pesticides	Dichlorodiphenytri- chloroethane (DDT), Aldrin/Dieldrin, Alpha HCH, Beta HCH, Chloropyriphos, Endosulfan (alpha, beta, and sulphate), Ethion, Alachlor, Atrazine, Butachlor, Delta HCH, 2,4-Dichlorophenoxyacetic acid
Specific Parameters	Dissolved Oxygen (DO), Mineral oil , Free Residual Chlorine, Biochemical Oxygen Demand (BOD), Total Pesticide Residue, Radio-active elements, Cyanide, Poly Aromatic Hydrocarbons (PAH), Total Organic Carbon (TOC), Chemical Oxygen Demand (COD), Polychlorinated Biphenyls, N-Nitro-sodi-methylamine (NDMA), Anionic Detergents (as MBAS), Oils & Grease, , Phenolic Compound (asC_6H_5OH), Trihalomethanes (Bromoform, Dibromo-methane, Bromodichloromethane, Chloroform), Methyl parathion, Gamma–HCH (Lindane), Phorate, Isoproturon, Malathion, Monocrotophos, Uranium

The major works on calculating or finding the water quality is done by laboratory methods and the parameters which are used are pH, DO, Turbidity, Nitrate, Phosphorous, Hardness, Faecal Pollution, Temperature, Residual Chlorine, Chloride, Fluoride, Iron, Ammonia, Alkalinity, etc.

2.3 SELECTION OF WATER QUALITY PARAMETERS

The selection of variables to be included in a water quality assessment must be related to the objectives of the water quality assessment program and the factors that depend on it. The parameters that are considered in the present study with a brief description for each one are listed below:

A. pH

The pH scale is a logarithmic scale with a range of 0 to 14, with 7 being regarded as neutral. Alkalinity is represented by numbers above 7, whereas acidity is represented by values below 7. The appropriate pH range for drinking water in India is normally between 6.5 and 8.5, as per BIS regulations. This range guarantees that the water is neither acidic nor alkaline.

B. Turbidity

Turbidity is the cloudiness of water. It is a measure of the ability of light to pass through water. The permissible limit for turbidity in water intended for domestic supplies is 5 nephelometric turbidity units (NTU). This limit ensures that the water is visually clear and free from suspended particles that can affect its aesthetic quality and potentially indicate contamination.

NTU is a unit of measurement commonly used to quantify the turbidity of water. It is based on the scattering of light by suspended particles in the water, with higher turbidity values indicating a greater concentration of particles.

C. Temperature

Temperature refers to the physical property that measures the degree of heat or coldness of water. It is typically measured in degrees Celsius (°C) and is an important parameter to consider in evaluating the suitability and comfort of water for consumption. The temperature is measured in situ, using a thermometer or thermistor. The acceptable temperature range for drinking water in India is typically between 10°C and 25°C. This range ensures that the water is within a comfortable and safe temperature for consumption.

D. Dissolved Oxygen (DO)

Dissolved oxygen (DO) plays a crucial role in assessing the quality of water in streams, rivers, and lakes. It serves as a vital indicator of water pollution, with higher concentrations of dissolved oxygen indicating better water quality. The acceptable level of dissolved oxygen should be adequate to sustain the aquatic life inhabiting the water body.

In general, for healthy aquatic ecosystems, the dissolved oxygen level should be above 4-5 mg/L (milligrams per liter). This range ensures that there is enough oxygen available to support the survival of aquatic organisms.

E. Total Suspended Solid (TSS)

Total Suspended Solids (TSS) refers to the concentration of solid particles that are suspended in water and are larger than 2 micrometers in size. These particles can include sediment, organic matter, and other materials that are not dissolved in the water. The permissible limit for Total Suspended Solids in drinking water is 10 mg/L (milligrams per liter). This limit ensures that the water is visually clear and free from excessive suspended particles, which can affect the aesthetic quality of the water and potentially indicate contamination.

F. Chlorophyll or Algae

Chlorophyll is a pigment found in plants and algae, and its presence in water is typically associated with the presence of algae or other photosynthetic organisms. The Central Pollution Control Board (CPCB) uses either visual observation of the algae or using Most Probable Number (MPN/ 100 ml). It should be less than 50.

G. Salinity

Salinity refers to the amount of dissolved salts present in a water body. High salt levels can be detrimental to freshwater plants and animals, rendering the water unsuitable for drinking, irrigation, and livestock. According to BIS 2009, the acceptable limit of salinity is 100 PPT. [14]

H. Coloured Dissolved Organic Matter

Coloured dissolved organic matter (CDOM) is the optically measurable component of the dissolved organic matter in water. CDOM naturally occurs in aquatic environments, mainly as a result of tannins generated through rotting waste. As CDOM increases, the hue of the water will shift from green to yellow-green to brown. The traditional method used are absorption (colour) and fluorescence. Aquatic biological activity may be severely influenced by CDOM.

2.4 LIMITATIONS

The present limitations of the impact of water quality are majorly focused on the reliability and accuracy of laboratory testing and instruments. Recent years saw the use of the standards set by WHO.

The COD and BOD calculations many times are inaccurate as different researchers use different empirical formulas and not following a standard process or guidelines.

With advancements in instrumentation that incorporate digital technologies to test water quality, different laboratories must procure equipments that can perform water quality testing for multiple parameters. These equipments would not only reduce the turn-around time for delivery of test results but also significantly increase the number of tests that can be done by the laboratory as well as bring down the human intervention. But procuring these instruments not only includes the purchase price of the instrument but also additional expenses such as installation, training, calibration, and maintenance. Limited budgetary resources may restrict the procurement of the desired instruments.

It is important to carefully select sampling locations to represent the study area adequately, but it may not be possible to capture all the spatial variability present. So, the spatial coverage of laboratory-based assessments is restricted by the use of discrete sampling spots thereby increasing the possibility of missing specific variations in water quality.

Single-time-point observations are sometimes unable to detect irregular or momentary shifts in the water quality metrics.

Sample collection, transport, processing, and data analysis are essential for laboratory analyses, and these procedures can be time and resource intensive. These are tedious processes and there is a chance of leakage of the stored sample containers which can seriously halt the extend the experiments. Along with the exposure to air, temperature fluctuations, or light exposure can cause chemical reactions or microbial growth, affecting the accuracy of the measurements.

Many laboratories test only the samples acquired by government agencies and some independent researchers or the general public have limited access to these laboratories for checking their area samples.

CHAPTER 3

DETAILED REVIEW OF EXISTING LITERATURE ON EXTRACTION OF WATER QUALITY PARAMETERS USING SATELLITE DATA

3.1 OVERVIEW

The assessment of the water quality is majorly done using specialized laboratory methods which are dependent on the collection of samples, a process that covers a smaller area and is costly & time-consuming. With the advancement in research works, the use of remote sensing particularly satellite plays a significant role in making it possible to conduct repeated, frequent observations throughout a wide study area or over a large water body, thereby making it feasible to recognize temporal and spatial alterations in indicators of water quality. Researchers can identify changes in the quality of water patterns, comprehend the effects of changes in land use, and evaluate the effectiveness of pollution control measures via the analysis of long-term satellite data. Water agencies are strongly urged to improve their on-site functioning along with the creation of geographically distributed maps of some metrics related to water quality, given the low operational costs associated with the use of freely available data from satellites. The estimation of the chlorophyll and the water surface temperature was the first motivation to determine if using the techniques of remotely estimating these variables can be determined or not. Recent research has demonstrated how to estimate several water quality indices using remote sensing techniques and has attempted to link those estimations to potential climate change implications.

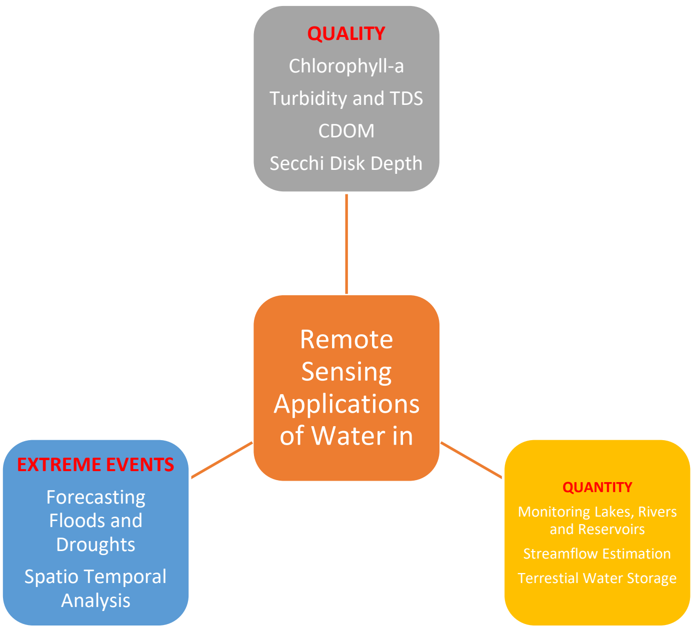

Fig. 3.1: A Diagram on Applications of Remote Sensing for Water

3.2 WORKS RELATED TO SATELLITE DATA IN WATER QUALITY

Different works using models, spectral indexes, using ML approaches have been used to find different parameters which provide accurate results but validation via the in-situ measurement has been a factor to consider in many studies.

Jerry C. Ritchie, et al. (2003) [15] used Landsat TMI data to find the aquatic vascular plants, suspended sediments (turbidity), algae/ chlorophyll. The research suggested the new satellites like EOS, Sea-WiFS, MOS, Ikonos and high spatial resolution hyperspectral sensors in the future will provide improvement to monitor water quality.

Zhubin Zheng, et al. (2015) [16] in Dongting Lake, China used different specifications of Landsat like MSS, TM, ETM^{+}, and OLI to find TSM with good results and suggested the approach can be used in other similar environments and ecological locations to explore their changes in patterns.

Jiang Chen, et al. (2017) [17] conducted a study in the Lake Huron areas where they employed OLI Landsat 8 to identify favorable distributions and changes in CDOM (Colored Dissolved Organic Matter). They made noteworthy observations, revealing the model's capacity to effectively utilize Landsat-8 for monitoring water quality on a significant regional level, offering detailed spatial information and frequent updates over time.

E. Terrence Slonecker, et al. (2015) [18] in New York and New Jersey Bays used the Landsat 8 for detection of the CDOM, DOM, Fluorescence post hurricane sandy. The research showed that the increased spectral resolution and synoptic coverage provided a means to detect and quantify changes to water quality parameters in major rivers and waterways more accurately. Also, suggested needs to establish the fundamental equations linking the remotely sensed data to the in-situ measurements.

Deeksha Katyal, et al. (2012) [19] used IRS LISS IV satellite of 2008 imagery and assess the Yamuna river with GIS integration to find pH, Turbidity, Temperature, Hardness, TDS, DO, BOD, OIP and recommend the use of OIP to illustrate the need for preventative measures and to increase the understanding of general water quality issues.

Abdelmalik K. W, (2018) [20] used ASTER terra data of the Qaroun Lake situated in the north eastern part of the Western Desert of Egypt. Using 18 samples out of which 15 used for model construction and 3 for obtaining model to calculate temperature, turbidity, Hydrogen ion concentration (pH), salinity, TDS, EC, Total alkalinity, TOC and Orthophosphorus. He illustrated and proved the presence of significant empirical relations between ASTER data and observed water quality parameters. The calculated parameters obtained from ASTER reflectance bands enabled an accurate prediction for the parameters based on the mathematical equations derived through regression analysis.

Ahmed El-Zeiny and Sameh El-Kafrawy (2016) [21] conducted a study in Burullus Lake, which is one of the largest lakes in northern Egypt. They utilized Landsat 8 OLI and a model generated through GIS to determine the levels of BOD, TN, and TP in the lake. The researchers applied previously developed empirical models for water quality analysis. Their findings demonstrated the significant contribution of remote sensing and GIS technologies in studying water quality, particularly the use of water quality empirical equations and GIS cartographic models. These tools play a crucial role in environmental management and assessment.

Vassiliki Markogianni, et al. (2018) [22] applied Landsat 8 OLI of 2014 along with the in-situ measurements in Trichonis Lake, Greece for estimating Chlorophyll-a, Ammonium Concentrations, and Total Phosphorous. The results showed a relatively variable statistical relationship between the in-situ and reflectance.

Ilhomjon Aslanov, et al. (2021) [23] calculated the soil salinity in the Fergana valley eastern part of Uzbekistan using Landsat 8 OLI. They conclude that using GIS and RS for soil salinity mapping provide higher degree of spatial accuracy and is extremely cost-effective.

Kaire Toming, et al. (2017) [24] used Sentinel-3 OLCI to calculate the CDOM, TSM and Chl-a at the Baltic Sea near Sweden. They advised Intercalibration of laboratory methods between different institutions to ensure validation of satellite products against data with well-characterized accuracy.

Wilaiporn Pimwiset, et al. (2022) [25] used mathematical equations along with the sentinel-2 to determine the water turbidity in the Chao Phraya River, Thailand. The estimation via the remotely sensed data has significant benefits for mapping and monitoring entire rivers by reducing the traditional process’s which are labour-intensive and time-consuming.

Muchlisin Arief (2015) [26] utilized Landsat-7 ETM+ to create models for assessing dissolved oxygen and temperature. The author's suggested approach of employing remote sensing satellites, particularly Landsat, offers significant potential for monitoring and mapping water quality in coastal areas. This method demonstrates notable efficiency when compared to conventional monitoring techniques.

A. KC, A. Chalise, et al, (2019) [27] conducted a water quality assessment of the Bijayapur River in Pokhara, Nepal, utilizing data from Landsat OLI/TIRS. Various correlation techniques were employed to establish the connection between optical and non-optical parameters. Additionally, regression techniques were utilized to determine the suitable relationship between band imagery and surface water quality parameters.

E. E. Cruz-Montes, et al. (2023) [28] applied remote sensing and multiple linear regression methods for water quality estimation for the DO, ph, turbidity and temperature using Landsat 8 OLI/TIRS data. The estimation through statistical models was a useful monitoring method and presented a good correlation between the in-situ values and those estimated for each water quality parameter for the field data collection date.

Linda Theres B, et al. (2022) [29] used Landsat 7 ETM+ and ASTER data in the Cauvery delta of Tamil Nadu to monitor water quality parameters like temperature, pH, Chi-square test, etc. They suggested that the hyperspectral imaging can be used to monitor and forecast water quality in the future through the development of a more precise mathematical relationship.

Nimisha Wagle, et al. (2019) [30] used Landsat 8 OLI along with the machine learning approach to estimate the DO and Chl-a for the Phewa Lake, located in the Kaski district of Nepal. They concluded that the machine learning techniques are better than the other regression analysis techniques as they used multiple variables to construct the best-fitting model.

Vaibhav Garga, et al. (2020) [31] used Sentinel-2 MSI to check the turbidity level in Ganga River at different locations during the covid-19 period and found different stretches of the river were having reduced levels of turbidity.

T. Seleem, et al. (2022) [32] used Landsat-8 OLI and Sentinel-2 TSM to monitor water quality in the Timsah Lake, Ismailia district, Egypt by using two approaches; semi-analytical and empirical modelling but there was a lack of ground truth for validation.

Fernanda M. C.et al. (2020) [33] in the Três Marias Reservoir of Brazil used Sentinel-2 MSI and Landsat-8 OLI to compare the performance of Sentinel-2's MSI and

Landsat-8’s OLI sensors for estimating water quality parameters through empirical statistical inference using regression.

N. Hussain, et al. (2017) [34] used Landsat 8 OLI to calculate the water quality in different sampling locations in Dhaka, Bangladesh. The research suggested some parameters of water quality were highly interrelated with the reflected sensors of the satellite and there was an interrelation between pH and Temperature.

3.3 APPLICATIONS, CHALLENGES, AND LIMITATIONS

This section focuses on the challenges, applications, and limitations associated with the use of satellite remote sensing for water quality measurements.

3.3.1 Applications

The major applications of satellite remote sensing in relation to water quality are as follows:

- Prediction of Water Quality Parameters
- Assessment of Water Pollution by Necessary Spectral Study in Rivers, Lakes, and Water Bodies
- Flood Mapping & Management
- Observation of Coastal Water Along the Rivers
- Detection of Total Dissolved Solids in Coastal Areas
- Assessment of Temporal Changes in Water Quality
- Water Quality Monitoring and Estimation
- Algal-bloom Detection
- Estimation of Bio-Physiological Parameters
- Estimation of Coloured Dissolved Organic Matter for Complex Inland Water

3.3.2 Challenges

- By analysing the electromagnetic energy that is reflected or transmitted from the Earth's surface, satellite sensors may identify water quality indicators due to atmospheric interference. Measurement precision, however, might be influenced by air interference, such as scattering and absorption. To reduce these errors, specialized atmospheric correction techniques are used.
- Satellite sensors have limitations in terms of their spatial and temporal resolution. While the time resolution might not be frequent enough to track quickly changing

conditions, the geographical resolution could not be sufficient to detect small-scale fluctuations in water quality.

- The accuracy and applicability of measurements of water quality might be impacted by the spectral capabilities and restrictions of various satellite sensors. Sensor calibration, spectral band selection, and sensor fusion techniques are used to overcome these difficulties.

3.3.3 Limitations

1. **Ground Truth Validation:** Water quality measurements taken directly from the water bodies must be compared with satellite-derived data. However, acquiring significant ground truth data can be expensive and logistically difficult, prompting challenges regarding the accuracy of satellite-based measurements.
2. **Impossible to Calculate All Parameters:** Although satellites can estimate several types of water quality parameters, some, including contaminants aren't easily measurable via remote sensing. A full assessment of water quality often necessitates additional in-situ observation and testing in the laboratory.
3. **Data Availability:** The availability of satellite data may be limited by issues including data costs, data scarcity, and distribution limitations. This might render it more difficult to use and apply satellite remote sensing for water quality monitoring, especially in places with poor infrastructure or resources.
4. **Weather Limitations:** Cloud cover, significant precipitation, and other extreme weather conditions might obscure satellite observations and reduce the availability of continuous water quality data. This may compromise the accuracy of long-term monitoring and obstruct real-time evaluations during urgent situations.

CHAPTER 4

TO ASSESS A RELATIONSHIP BETWEEN THE GROUND-BASED DATA AND THE DN VALUE AVAILABLE FROM SATELLITE DATA FOR YAMUNA RIVER

4.1 OVERVIEW

This study intends to examine the relationship between ground-based data and the Digital Number (DN) values for the Yamuna River, which are obtained through satellite photography. By building a connection between these two data sources, we may learn more about the viability of integrating satellite data as a reliable source for tracking certain features of the Yamuna River. Landsat 8/9 and Sentinel-2 satellite are in consideration as the majority of the studies are conducted using these two satellites globally. With the freely available data at 30 M resolution, these two satellites are considered for the present study.

4.2 STUDY AREA

The Ganga River's greatest tributary, the Yamuna River, is 1376 km long. It begins at the Yamunotri glacier, which is located close to the Banderpunch peaks of the lower Himalayas (38o 59' N and 78o 27' E) in the Mussoorie range, at an elevation of around 6387 meters above mean sea level in the Uttarkashi district of Uttarakhand. The river then travels through seven states. According to CPCB (2006), the overall catchment basin area of the river is 3, 66,223 km^2 (including the area of the Yamuna River itself, which is 20,375 km^2), or 42.5% of the Ganga basin and 10.7% of the country's total geographical landmass.

Several locations have been selected along the coast of the Yamuna River for the collection of water samples after a thorough analysis of satellite images and Google Earth Observations. The 27 different locations covered in this study commence at Hathnikund Barrage and ends at Hathi Ghat. Landsat 8/9 OLI data path 145, 146 & 147 rows 039, 040, and 041 are used to define the study area. The Sentinel-2 satellites 14 different tiles of the same locations as the Landsat are also used. Table 4.3 and 4.4 below shows the location of the satellite images along with their acquisition time:

Table 4.1: Reference of Locations

ID	Locations	Longitude	Latitude
1	Hathnikund Barrage	77°34'59.52"E	30°18'48.30"N
2	Yamuna Ghat near Samalkha Bridge Sonipat	77° 7'58.18"E	29°15'1.29"N
3	Yamuna Ghat, Hathwala Gav, Panipat (HR)	77° 8'6.67"E	29°13'27.02"N
4	Signature Bridge 1 Km Downstream Wazirabad Bridge	77°13'50.57"E	28°42'24.99"N
5	Majnu ka Tilla Near Gurudwara	77°13'45.17"E	28°41'46.11"N
6	DC Boat Club near Chandigram Akhada	77°13'53.36"E	28°40'44.18"N
7	Pillar No 6 ISBT Bridge Delhi	77°14'2.91"E	28°40'16.37"N
8	Balaknath Mandir near Ganesh Ghat no 24	77°14'19.92"E	28°39'58.26"N
9	Old Iron Bridge New Delhi (near CWC Tower)	77°14'45.53"E	28°39'44.52"N
10	Geeta Colony Bridge	77°15'43.27"E	28°39'5.92"N
11	Gorakhnath Dhuna Ashram	77°15'52.76"E	28°38'35.25"N
12	Delhi Sachivalaya Upstream of ITO Bridge 700m	77°15'27.02"E	28°38'1.08"N
13	Kailash Nagar Bhimdal Akhada	77°15'5.96"E	28°39'43.66"N
14	Chhath Ghat Downstream Old Bridge	77°15'11.98"E	28°37'35.50"N
15	Kalindi Kunj 500m Upstream Biodiversity Park	77°17'34.37"E	28°34'22.82"N
16	Midstream Kalindi Kunj Biodiversity Park	77°17'40.39"E	28°34'10.45"N
17	Downstream 600m of Kalindi Kunj Biodiversity Park	77°17'47.37"E	28°33'49.75"N
18	Cheer Ghat neat Banke Bihari Temple Mathura	77°41'46.97"E	27°35'10.16"N
19	Vishram Ghat near Kans Qila Mathura	77°41'21.43"E	27°30'9.00"N
20	Brahmand Ghat Mathura Downstream of Refinery Mathura	77°44'40.84"E	27°25'1.17"N
21	Downstream of Barrage Ghat	77°42'49.47"E	27°26'33.35"N
22	Gokul Ghat Mathura Cantt.	77°42'48.77"E	27°27'31.62"N
23	Poiya Ghat, Sikandra, Agra	78° 1'19.03"E	27°15'17.05"N
24	Balkeshwar Ghat, Agra	78° 1'53.23"E	27°13'21.38"N
25	Water Works Ghat Agra	78° 2'3.97"E	27°12'16.52"N
26	Itmad-du-Daula Ghat, near Bridge Agra	78° 1'48.64"E	27°11'35.80"N
27	Hathi Ghat Near Agra Fort	78° 1'42.69"E	27°11'6.39"N

Table 4.2: Reference of Ground Truth for Validation

ID	Longitude	Latitude	pH	Turbidity	DO	TDS	Temperature
1	77°34'59.52"E	30°18'48.30"N	9.4	0	11.1	224	24.5 °C
2	77° 7'58.18"E	29°15'1.29"N	9.1	35	5.4	669	25.8 °C
3	77° 8'6.67"E	29°13'27.02"N	8.8	30	2.6	798	28 °C
4	77°13'50.57"E	28°42'24.99"N	7.8	70	0.2	1470	24.5 °C
5	77°13'45.17"E	28°41'46.11"N	7.8	65	0.4	1480	24.6 °C
6	77°13'53.36"E	28°40'44.18"N	7.7	95	0.2	1500	24.8 °C
7	77°14'2.91"E	28°40'16.37"N	7.8	70	0.2	1590	24.5 °C
8	77°14'19.92"E	28°39'58.26"N	7.8	60	0.1	1510	24.8 °C
9	77°14'45.53"E	28°39'44.52"N	7.7	80	0.1	1530	24.9 °C
10	77°15'43.27"E	28°39'5.92"N	7.8	65	0.3	1530	25.8 °C
11	77°15'52.76"E	28°38'35.25"N	7.8	60	0.1	1440	25.8 °C
12	77°15'27.02"E	28°38'1.08"N	7.9	60	0	1530	36.8 °C
13	77°15'5.96"E	28°39'43.66"N	8	85	0.1	1330	26.9 °C
14	77°15'11.98"E	28°37'35.50"N	7.7	50	0.3	1500	26.2 °C
15	77°17'34.37"E	28°34'22.82"N	7.8	60	0.2	1610	28.5 °C
16	77°17'40.39"E	28°34'10.45"N	7.9	28	0.2	777	27.2 °C
17	77°17'47.37"E	28°33'49.75"N	7.9	30	0.8	494	26.2 °C
18	77°41'46.97"E	27°35'10.16"N	8.5	15	1.5	1220	28.8 °C
19	77°41'21.43"E	27°30'9.00"N	8.3	22	2.3	1220	26 °C
20	77°44'40.84"E	27°25'1.17"N	8.4	22	2.8	1220	28.5 °C
21	77°42'49.47"E	27°26'33.35"N	8.4	22	1.8	1500	26.1 °C
22	77°42'48.77"E	27°27'31.62"N	8.4	35	1.9	1390	27.9 °C
23	78° 1'19.03"E	27°15'17.05"N	8.5	60	6.3	1410	28.1 °C
24	78° 1'53.23"E	27°13'21.38"N	8.3	115	0	1632	30.5 °C
25	78° 2'3.97"E	27°12'16.52"N	8.7	95	5.1	1400	28.3 °C
26	78° 1'48.64"E	27°11'35.80"N	2.6	100	3.7	1400	28.1 °C
27	78° 1'42.69"E	27°11'6.39"N	8.5	100	2.4	1330	28.5 °C

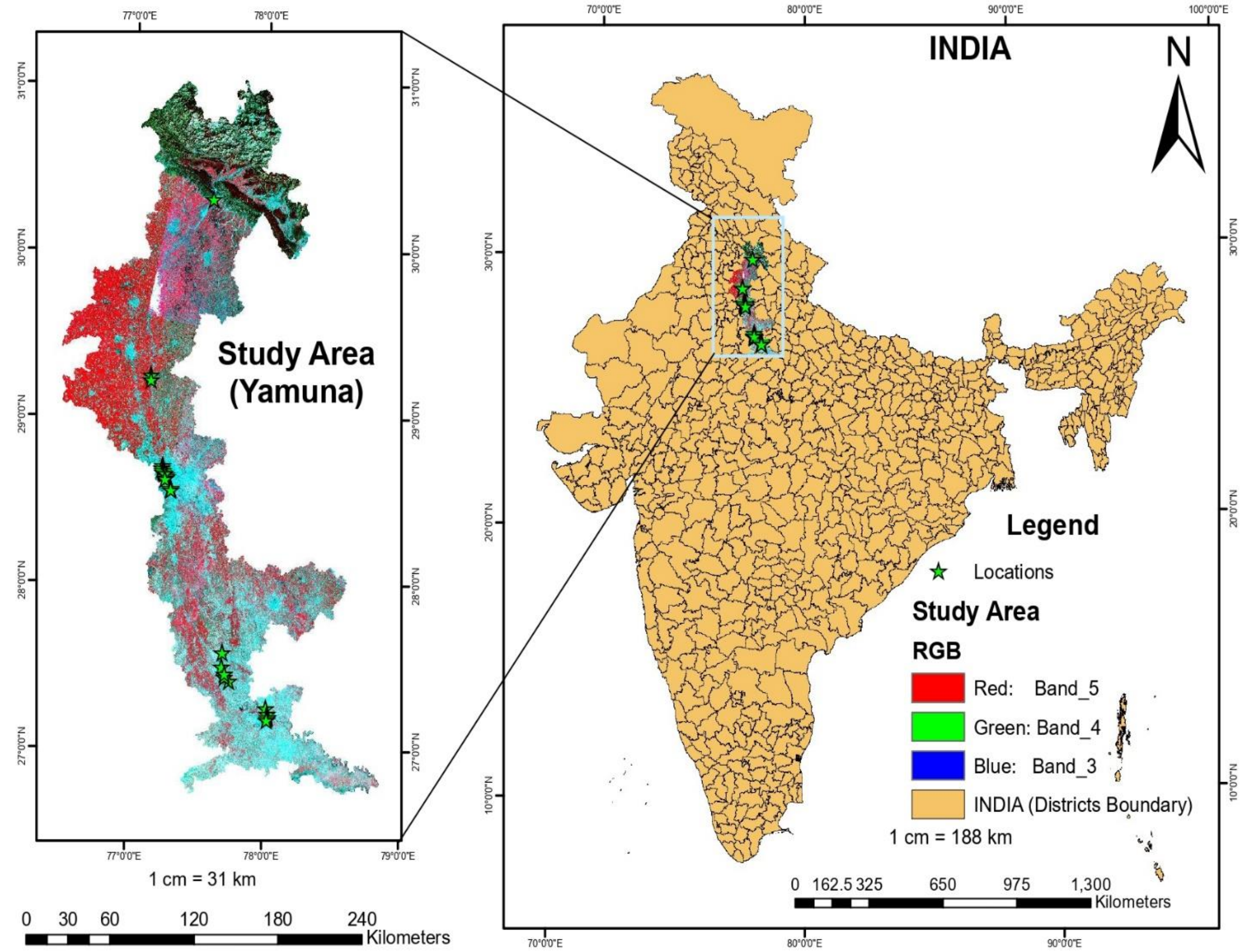

Fig. 4.1: Study Area Map

4.3 DATA USED

Landsat 8/9 OLI data path 145, 146 & 147 rows 039, 040, and 041 are used to define the study area. The table below shows the Landsat satellite image along with their acquisition time. Using standard band detection and the NDWI (Normalised Difference Water Index) methodology, the Landsat OLI's DN (digital number) value was determined. The reflection and absorption properties of water have an impact on the DN values of Landsat OLI. The NIR (near-infrared) spectrum is more readily absorbed by water and dissolved materials, while water and dissolved materials exhibit increased reflection in the green band. The NDWI model was used to evaluate the water quality.

$$NDWI = (GREEN - NIR)/(GREEN + NIR) \quad \text{-Eq. (4.1)}$$

Table 4.3: Reference of Landsat Satellite Image

ID	Satellite Image	Date of Acquisition
1	LC08_L2SP_146039_20230218_20230223_02_T1	18-02-2023
2	LC09_L2SP_146040_20230314_20230316_02_T1	14-03-2023
3	LC09_L2SP_146041_20230314_20230316_02_T1	16-03-2023
4	LC08_L2SP_145041_20230315_20230321_02_T1	15-03-2023
5	LC09_L2SP_147039_20230305_20230308_02_T1	08-03-2023
6	LC09_L2SP_147040_20230305_20230308_02_T1	05-03-2023

Table 4.4: Reference of Sentinel-2 Satellite Image

ID	Satellite Image	Date of Acquisition
1	S2A_MSIL2A_20230310T052641_N0509_R105_T43RFM_20230310T093103.SAFE	10-03-2023
2	S2A_MSIL2A_20230310T052641_N0509_R105_T43RFN_20230310T093103.SAFE	10-03-2023
3	S2A_MSIL2A_20230310T052641_N0509_R105_T43RFP_20230310T093103.SAFE	10-03-2023
4	S2A_MSIL2A_20230310T052641_N0509_R105_T43RFQ_20230310T093103.SAFE	10-03-2023
5	S2A_MSIL2A_20230310T052641_N0509_R105_T43RGK_20230310T093103.SAFE	10-03-2023
6	S2A_MSIL2A_20230310T052641_N0509_R105_T43RGL_20230310T093103.SAFE	10-03-2023
7	S2A_MSIL2A_20230310T052641_N0509_R105_T43RGM_20230310T093103.SAFE	10-03-2023
8	S2A_MSIL2A_20230310T052641_N0509_R105_T43RGN_20230310T093103.SAFE	10-03-2023
9	S2A_MSIL2A_20230310T052641_N0509_R105_T43RGP_20230310T093103.SAFE	10-03-2023
10	S2A_MSIL2A_20230310T052641_N0509_R105_T43RGQ_20230310T093103.SAFE	10-03-2023
11	S2A_MSIL2A_20230310T052641_N0509_R105_T44RKU_20230310T093103.SAFE	10-03-2023
12	S2B_MSIL2A_20230312T051659_N0509_R062_T44RKQ_20230312T084709.SAFE	12-03-2023
13	S2B_MSIL2A_20230312T051659_N0509_R062_T44RKR_20230312T084709.SAFE	12-03-2023
14	S2B_MSIL2A_20230312T051659_N0509_R062_T44RKS_20230312T084709.SAFE	12-03-2023

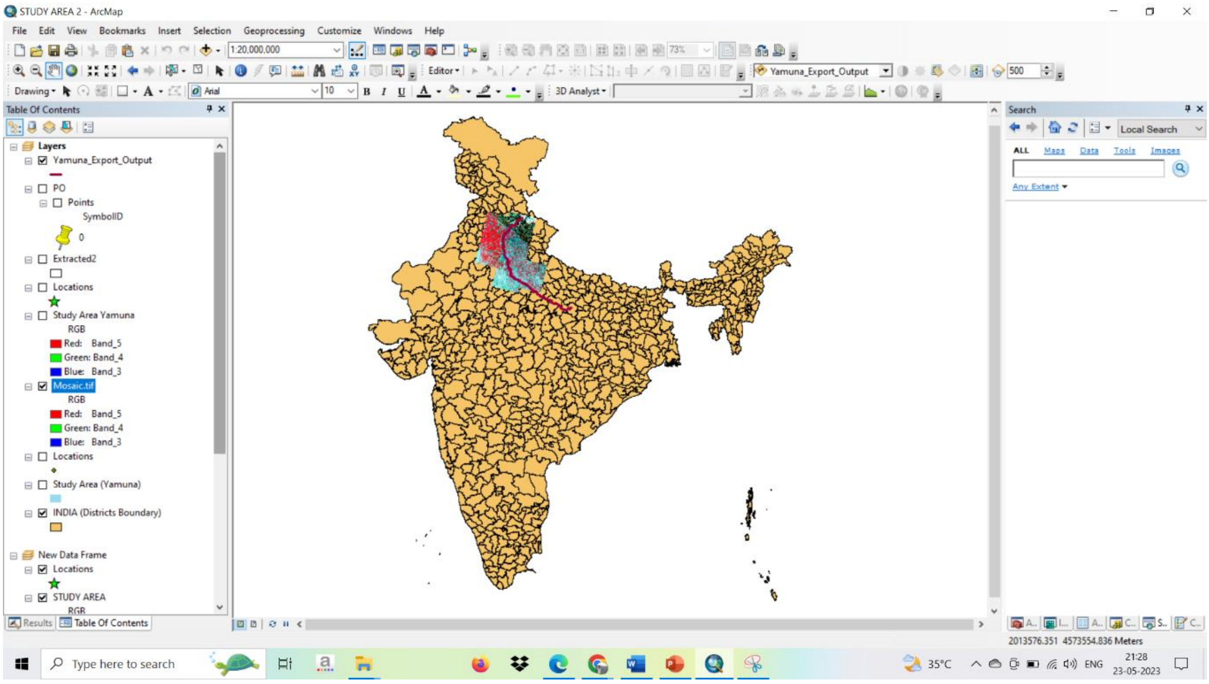

Fig. 4.2: Landsat tiles opened in ArcMap along with the boundaries and river shapefile

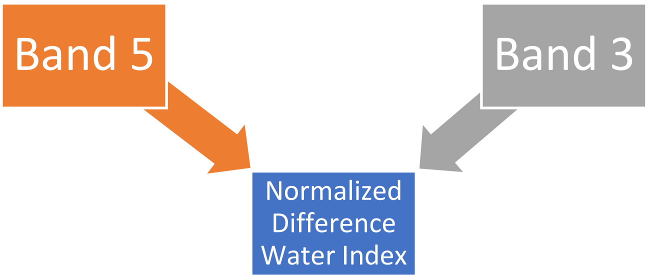

Fig. 4.3: NDWI Methodology

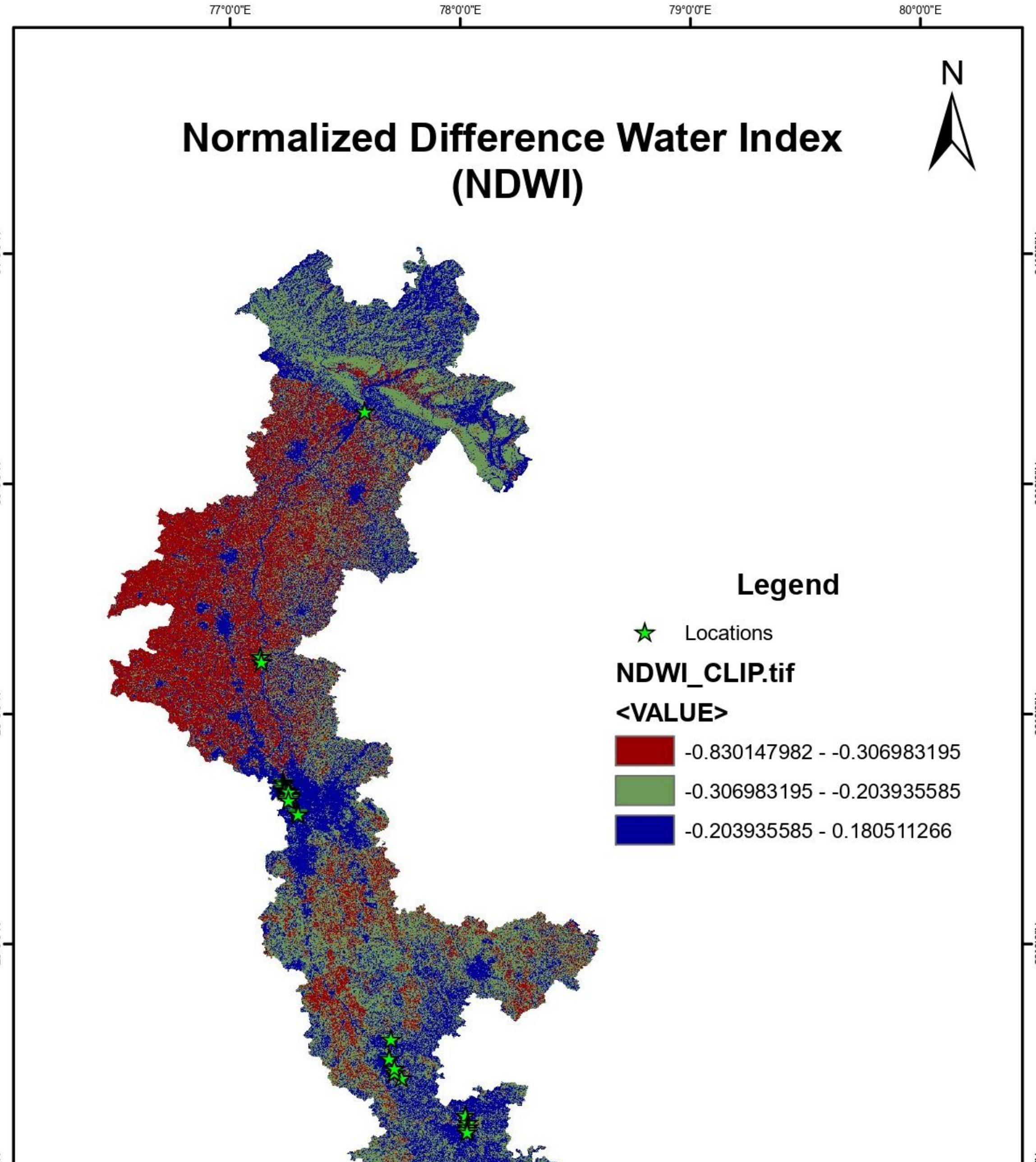

Fig. 4.4: NDWI Map

The Survey of India's Online Maps Portal supplied the necessary shapefile containing administrative boundaries for various states across the entire country, including districts, at a high-quality scale of 1:1M. This dataset serves as a comprehensive database encompassing administrative boundaries at the district level, including state and district boundaries, for the entire country.

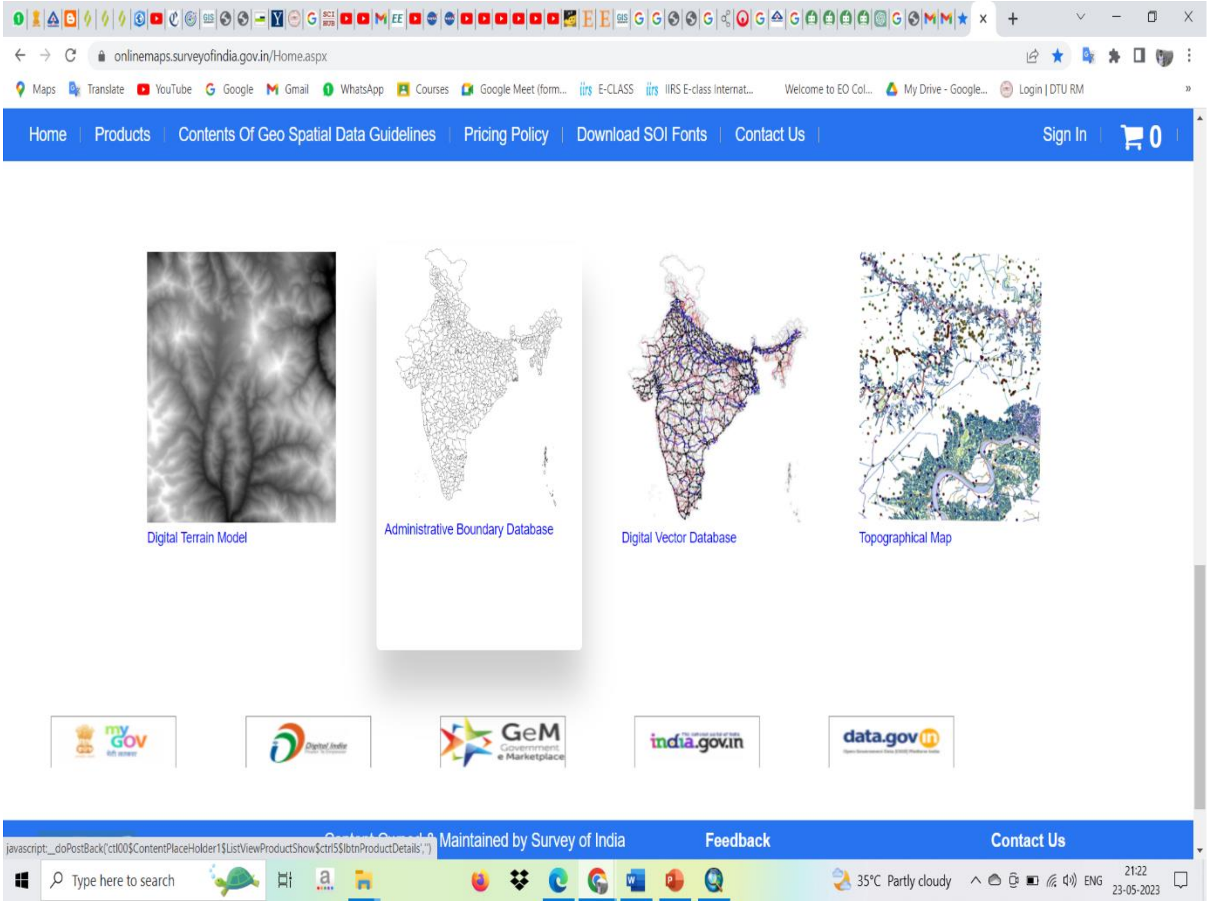

Fig. 4.5: Online Maps Portal

The Open Government Data Portal developed and hosted by the National Informatics Centre (NIC) provided the required digitized shapefile of the Yamuna River for reference.

The ArcMap 10.8 was used for the pre-and post-processing of the datasets along with the use of different model algorithms in the raster calculator function to calculate the desired results.

4.4 METHODOLOGY

After the selection of the parameters to calculate, different approaches for different parameters were applied after a thorough review of different publications. The reviewed studies mainly focus on some specific parameters in a relatively smaller part of the areas majorly the lakes and generally do not cover any state entirely. The parameters used are not consistent with all the studies as major researchers were considered either using 8 or 10 parameters.

The approaches used for the different parameters are listed below:

Table 4.5: Algorithms Used for Model Builder

S. No	PARAMETER	MODEL ALGORITHM
1	pH [33]	9.9977 + (-110.1097 * B1) + (17.4231 * B3) + (49.6782 * B5)
2	Salinity [23]	(Green - SWIR)/ (Green + SWIR)
3	Turbidity [33]	0.2294 + (-59.2739 * B1) + (48.0012 * B3)
4	Land Surface Temperature [35]	$TOA = M_L * Q_{cal} + A_L$ $BT = (K_2 / (\ln (K_1 / L) + 1)) - 273.15$ $NDVI$ = (NIR -R)/(NIR+R) P_V = Square $((NDVI - NDVI_{min}) / (NDVI_{max} - NDVI_{min}))$ $\varepsilon = 0.004 * P_v + 0.986$ $LST = (BT / (1 + (0.00115 * BT / 1.4388) * Ln(\varepsilon)))$
5	Chlorophyll [27]	(NIR− red)/ (NIR + red)
6	Suspended Matters or Total Dissolved Solids [37]	-3311.4364+41.3237*B4-0.0779*B3*B4+0.00006353*B2*B3*B4
7	Dissolved Organic Matter or Coloured Dissolved Organic Matter [36]	23.65- (0.3528*band 1) - (0.657*band 2)
8	Dissolved Oxygen [33]	9.2505 + (-171.0251 * B2) + (236.9708 * B4) + (76.8288 * B6) + (-150.7815 * B11)

Using the model builder and the raster calculator function in the ArcMap Software, the tile-by-tile sections of the satellite are processed and then mosaiced to form a new raster file. After that the state boundary shapefile is used to extracted the desired area parallel to the flowing river using the river shapefile for reference. Using the KML to layer function in the ArcMap, the 27 locations are changed to a layer shapefile to extract the values of the pixel for the processing. The location layer file is automatically georeferenced using the Google Earth Pro software as the conversion tool function process the file in the same coordinate system as the satellite dataset. Finally, using the multi value extraction tool the values are obtained and different graphs and results are generated.

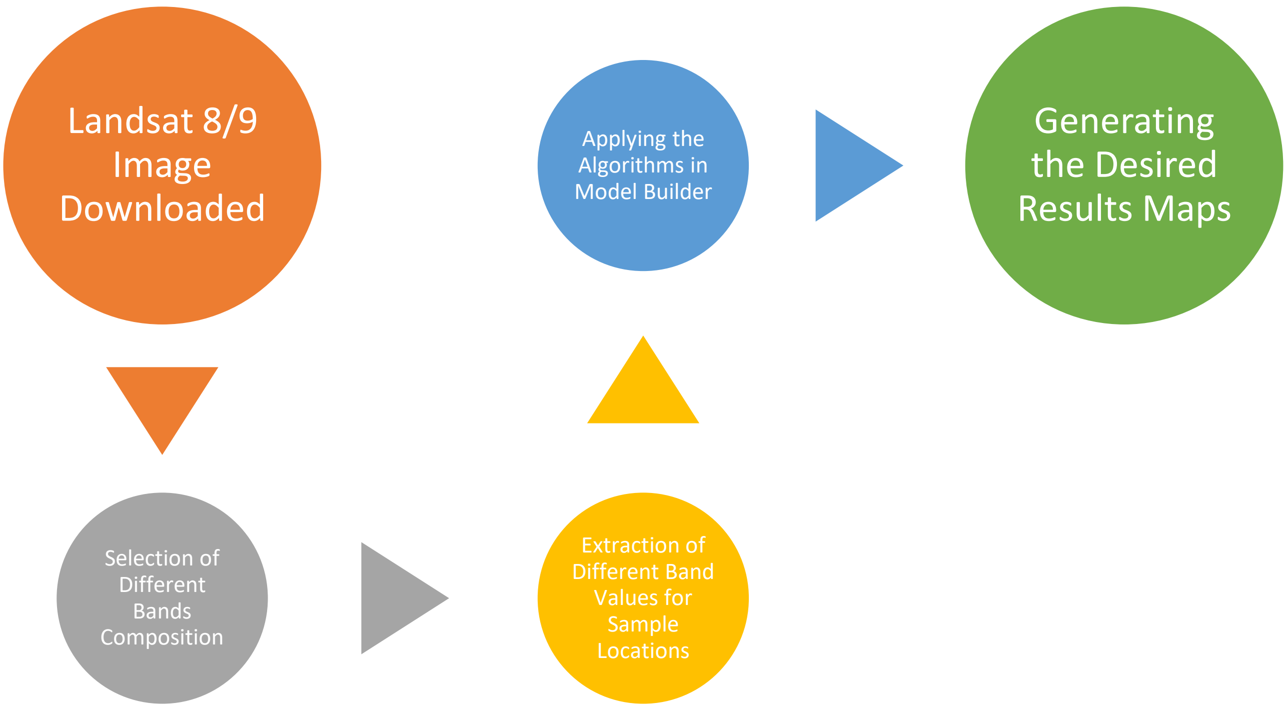

Fig. 4.6: General Methodology Applied for Maps Generation

4.5 RESULTS

A. pH

The model builder function is used to calculate ph. The combination of the Coastal/Aerosol, Green and Near Infrared bands in Landsat are used and the tile-by-tile process is applied by the model algorithm and then mosaiced and equalized to generate better results. The manual reclassification is used to normalize the pixel values accordingly and then the graph is generated and map is exported.

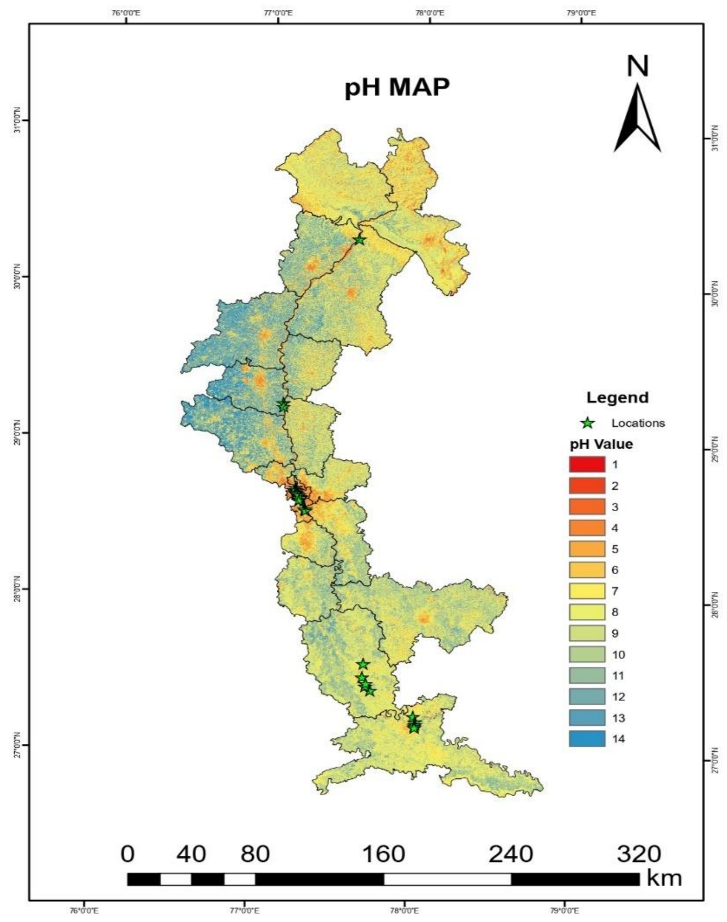

Fig. 4.7: Model Generated Map

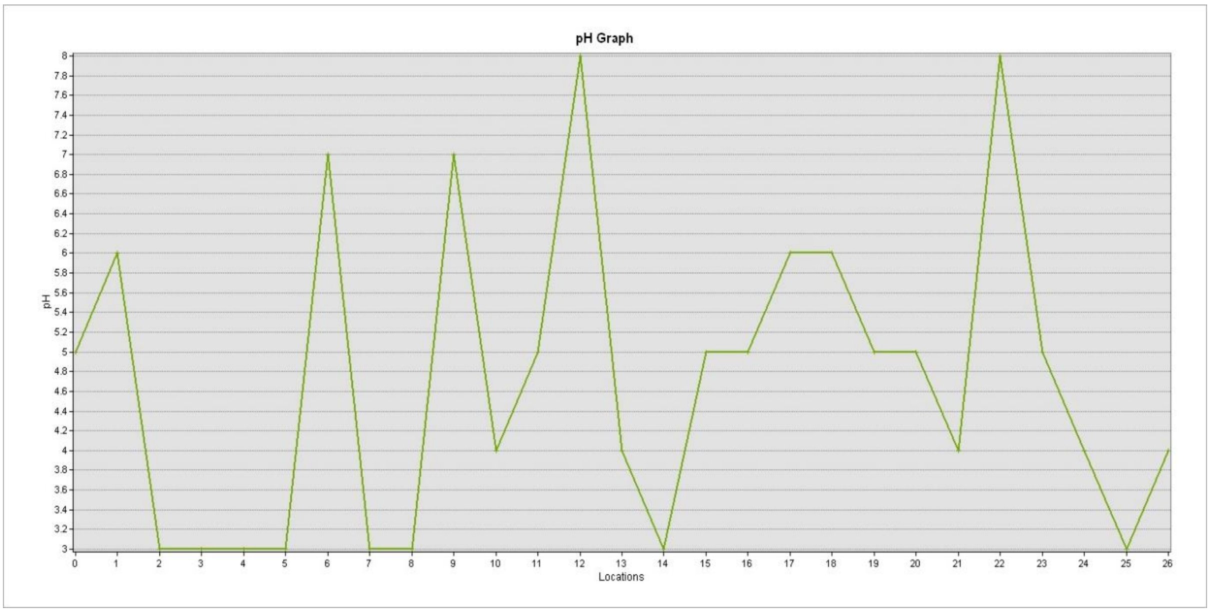

Fig. 4.8: Generated pH Graph

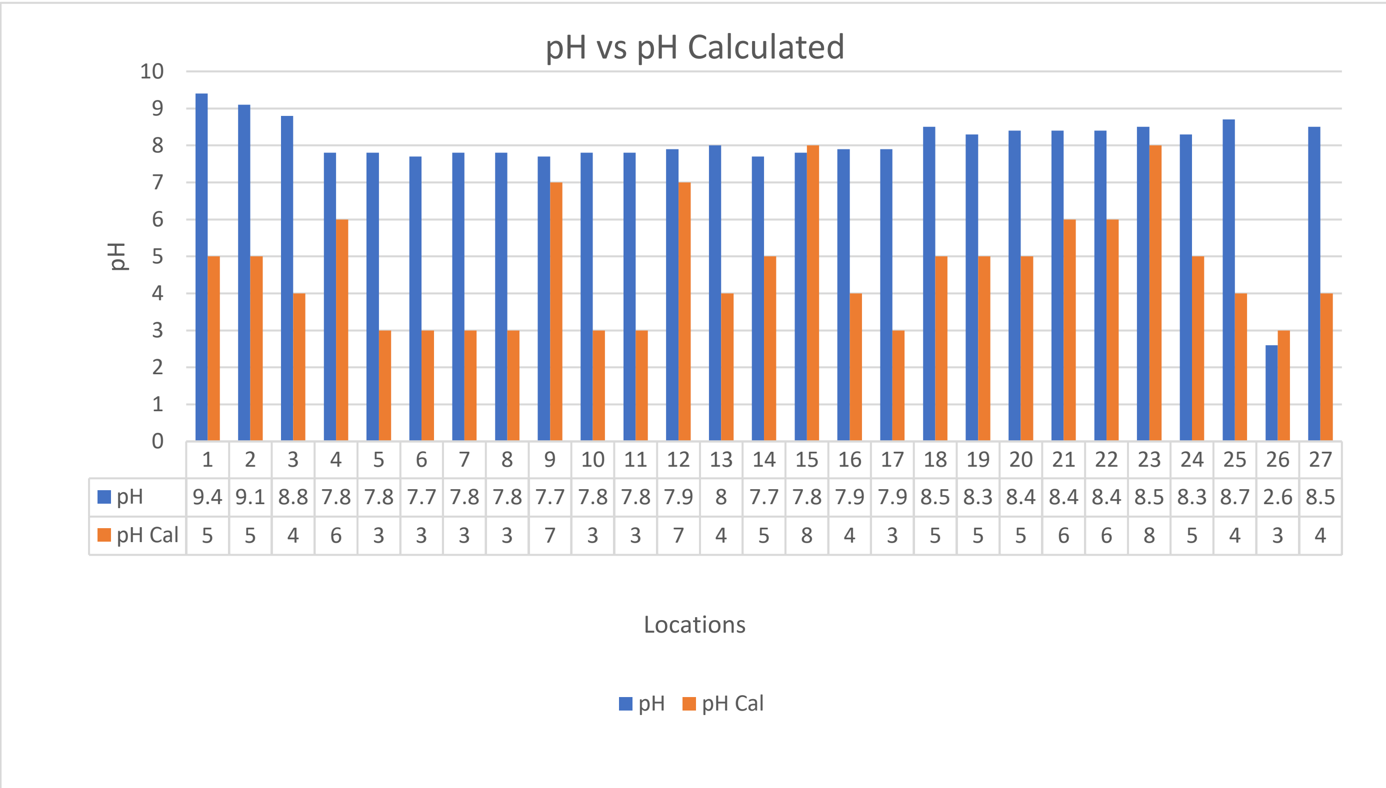

Fig. 4.9: pH (in-situ) vs pH (sat)

B. Salinity

The combination of the Green and SWIR band in landsat are used and the tile-by-tile process is applied by the model algorithm and then mosaiced and equalized to generate better results for the NDSI or Normalized Difference Soil Index. The manual reclassification is used to normalize the pixel values accordingly and then the graph is generated and map is exported. The NDSI is divided into 4 classes to better understand the results.

Table 4.6: Range of NDSI Classes

Classes	Level of Salinization
< 0.16	Low
0.16 – 0.50	Medium
0.50 – 1.50	High
1.50 – 3.00	Very High

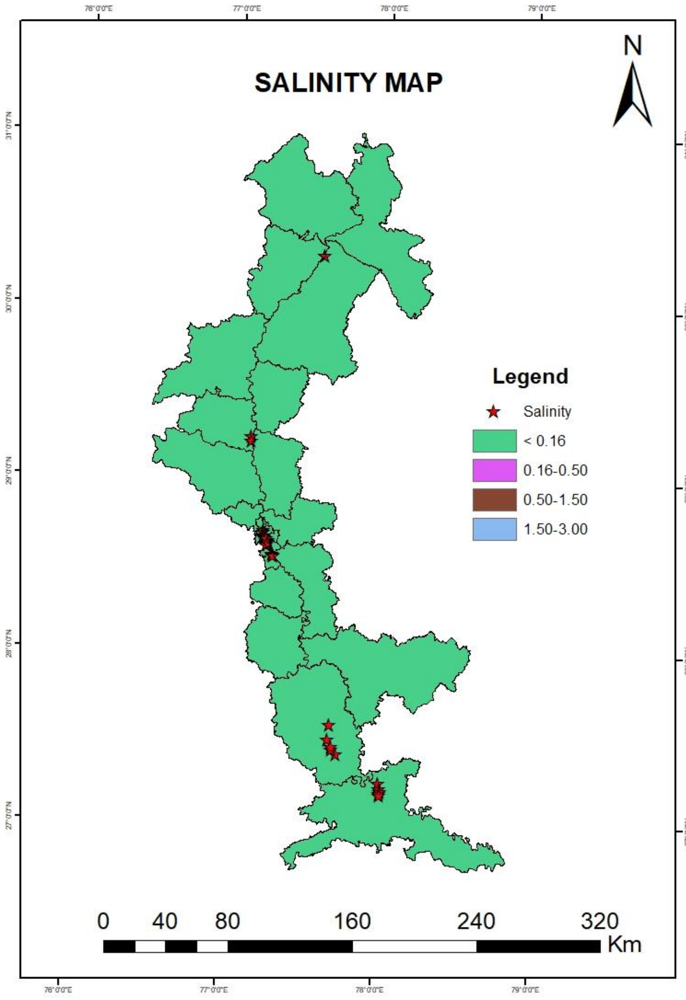

Fig. 4.10: Salinity Map

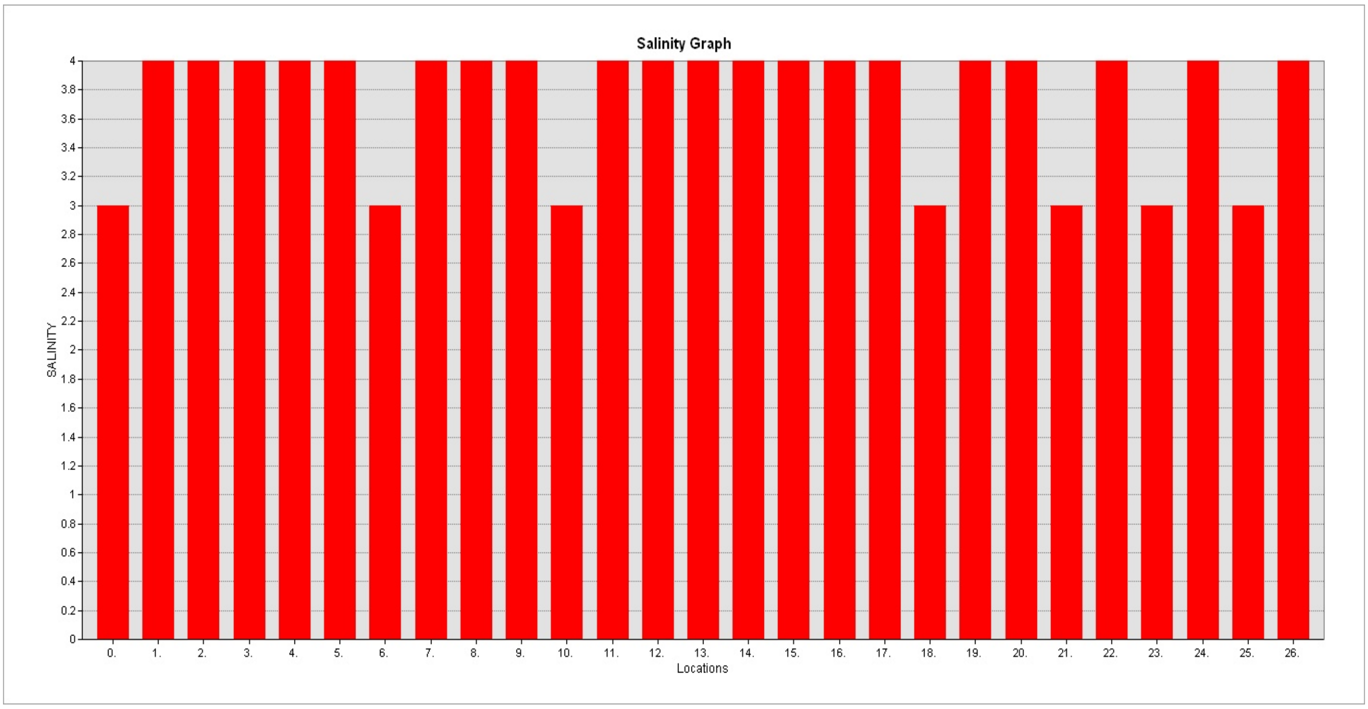

Fig. 4.11: Salinity Graph

C. Turbidity

The combination of the Coastal/Aerosol and Green band in landsat are used and the tile-by-tile process is applied by the model algorithm equation mentioned below and then mosaiced and equalized to generate better results for the turbidity map. The manual reclassification is used to normalize the pixel values accordingly to the mentioned ranges in the Indian IS Code for turbidity and then the graph is generated and map is exported. Range in NTU for turbidity is divided into 7 classes accordingly for understanding.

Table 4.7: Range of Turbidity in NTU

Range	**Nearest Recorded**
0 – 1	0.05
1 – 10	0.1
10 – 40	1
40 – 100	5
100 – 400	10
400 – 1000	50
Greater than 1000	100

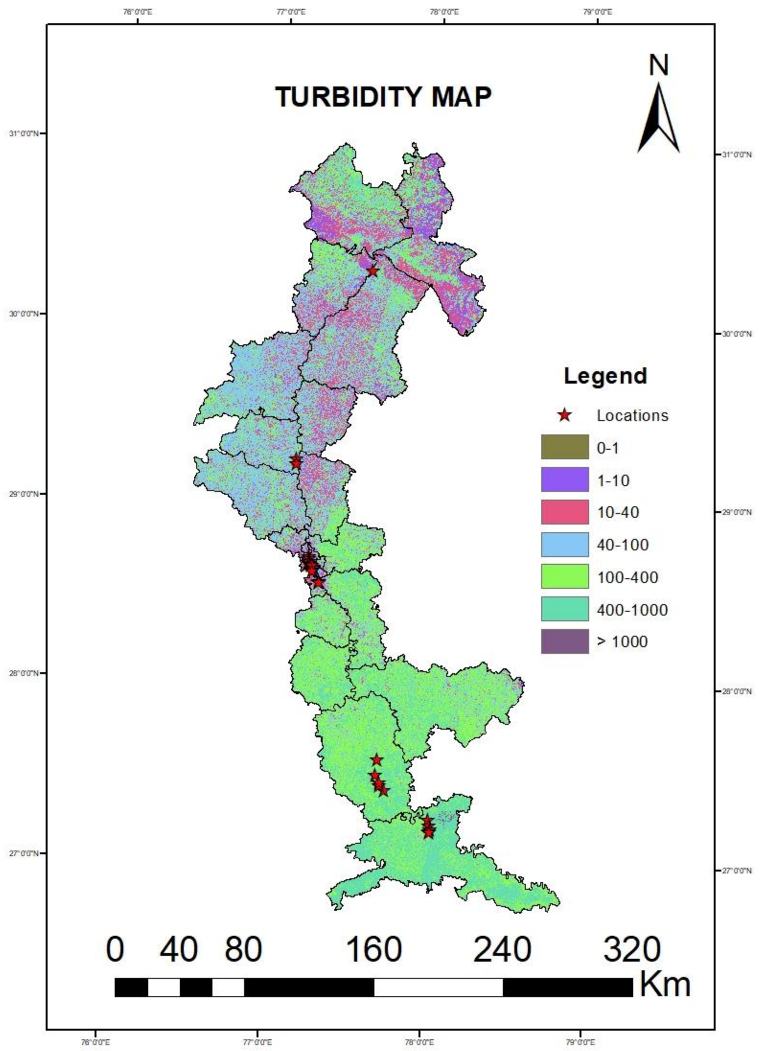

Fig. 4.12: Turbidity Map

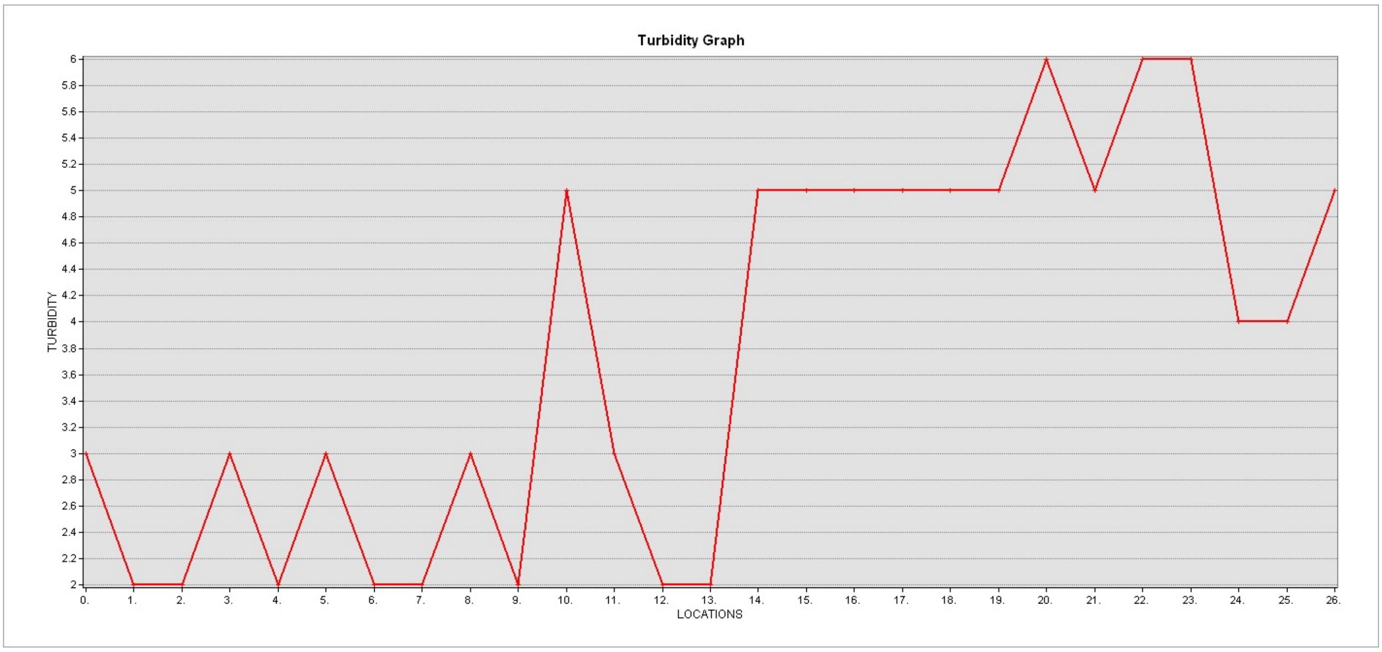

Fig. 4.13: Turbidity Graph

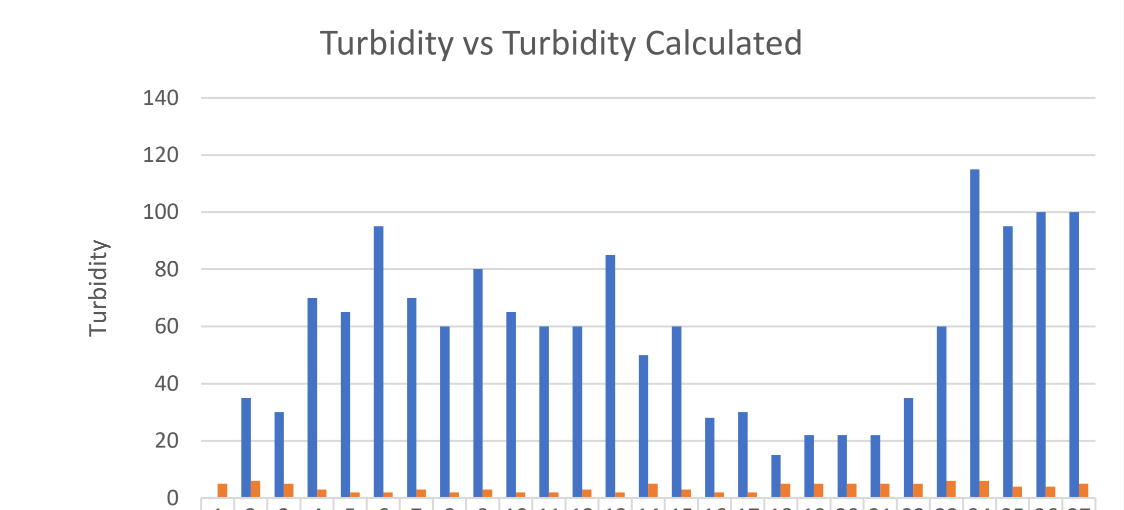

	1	2	3	4	5	6	7	8	9	10	11	12	13	14	15	16	17	18	19	20	21	22	23	24	25	26	27
Turbidity	0	35	30	70	65	95	70	60	80	65	60	60	85	50	60	28	30	15	22	22	22	35	60	11	95	10	10
Turbidity Cal	5	6	5	3	2	2	3	2	3	2	2	3	2	5	3	2	2	5	5	5	5	5	6	6	4	4	5

Fig. 4.14: Turbidity (in-situ) vs Turbidity (sat)

D. Land Surface Temperature

Specific bands from Landsat 8 can be used to calculate the land surface temperature (LST). In particular, band 10's thermal function is used for this, while bands 4 and 5 are used to calculate the Normal Difference Vegetation Index (NDVI). However, the LST computation only uses the dataset that is currently available when a section or tile of data for the same date is absent. The methodology explains how to use ArcMap's Raster Calculator tool for this operation.

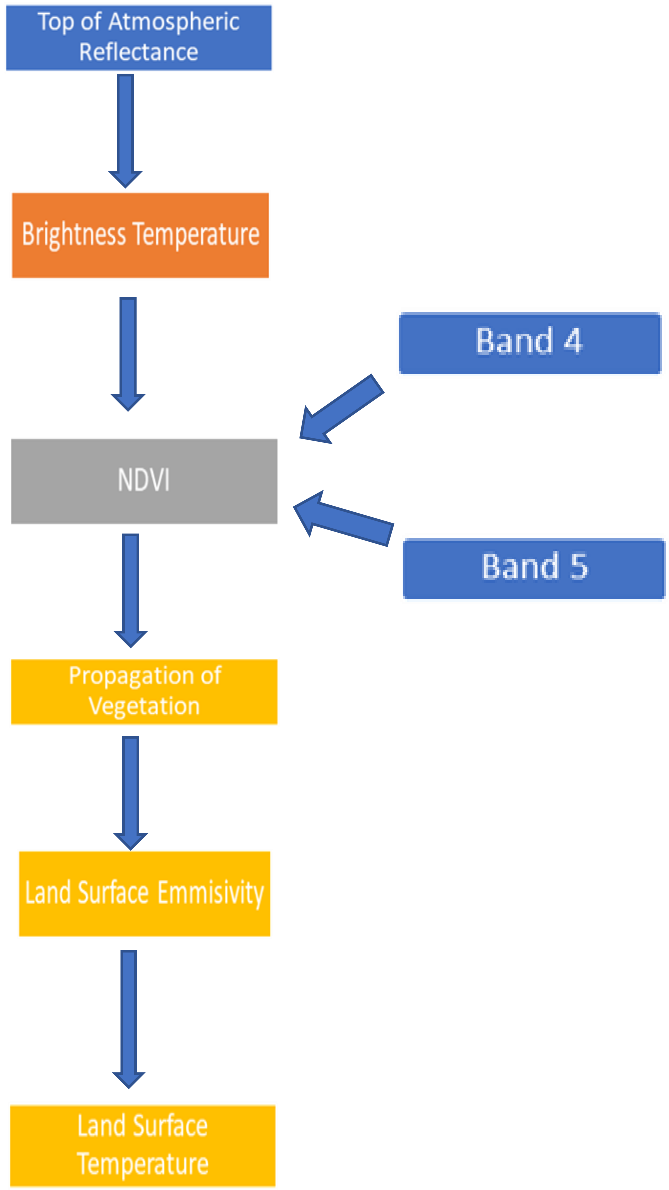

Fig. 4.15: Land Surface Temperature Methodology

- **Calculation of TOA (Top of Atmospheric) spectral radiance:**
- **Convert TOA values to Brightness Temperature (BT):**

  To obtain the results in Celsius, the radiant temperature is adjusted by adding the absolute zero (approx. -273.15°C).

- **Calculating NDVI:**
- **Calculate the proportion of vegetation (P_V):**
- **Calculate Emissivity (ε):**

  The value of 0.986 corresponds to a correction value of the equation.

- **Calculate the Land Surface Temperature (LST):**

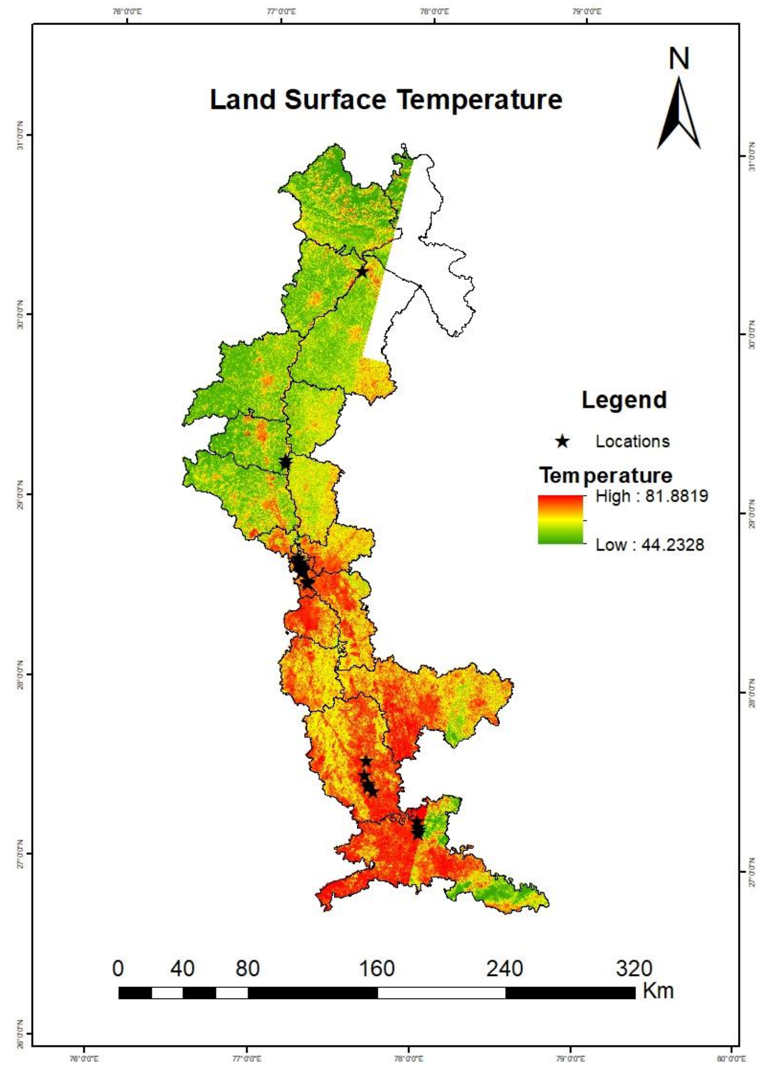

Fig. 4.16: Land Surface Temperature Map

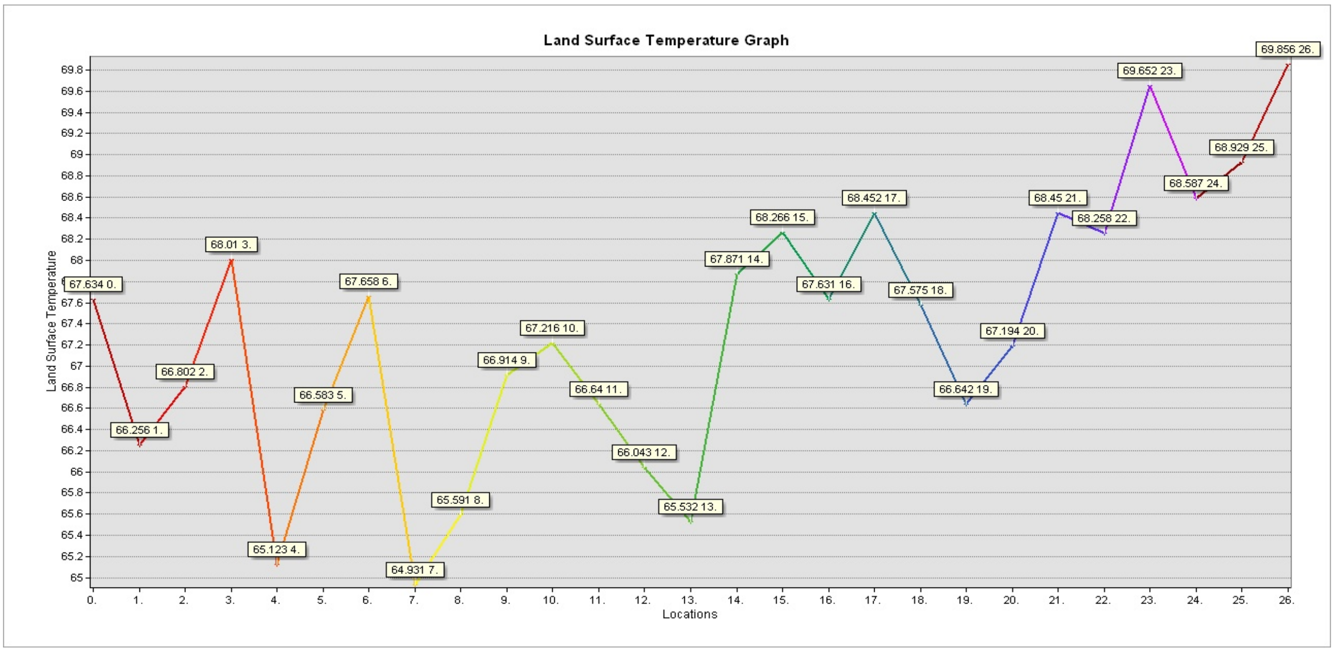

Fig. 4.17: Land Surface Temperature Graph

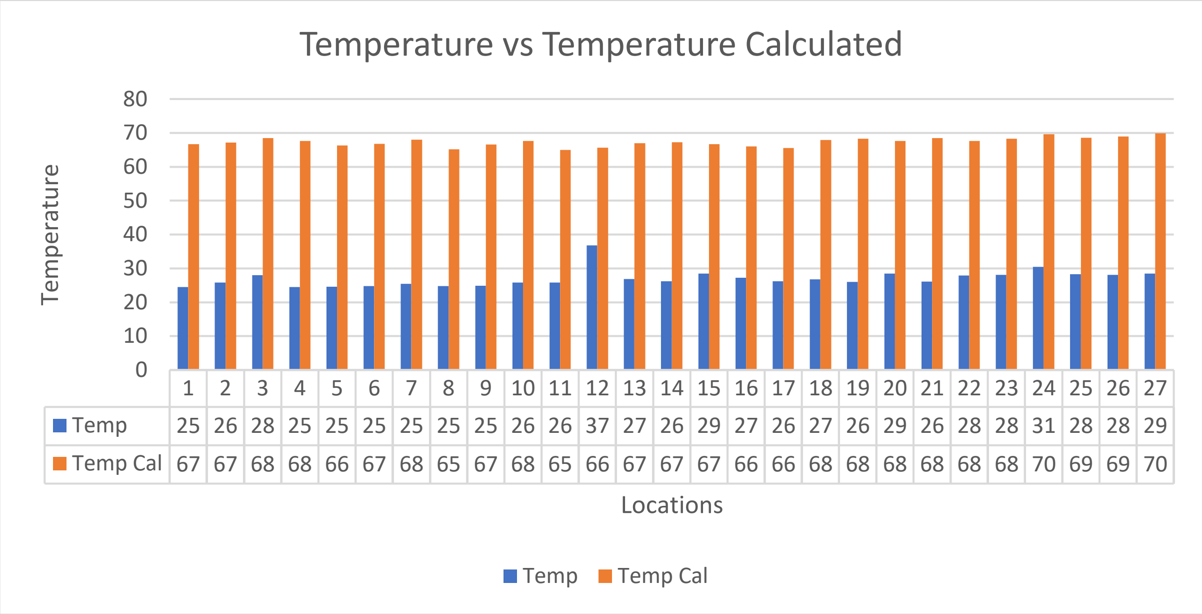

Fig. 4.18: Temperature (in-situ) vs Temperature Calculated

E. Chlorophyll

The Chlorophyll can be calculated using the Landsat 8 bands. In particular, bands 4 and 5 which are the RED and NIR bands respectively are used to calculate the NDVI which in turn is used to calculate the chlorophyll.

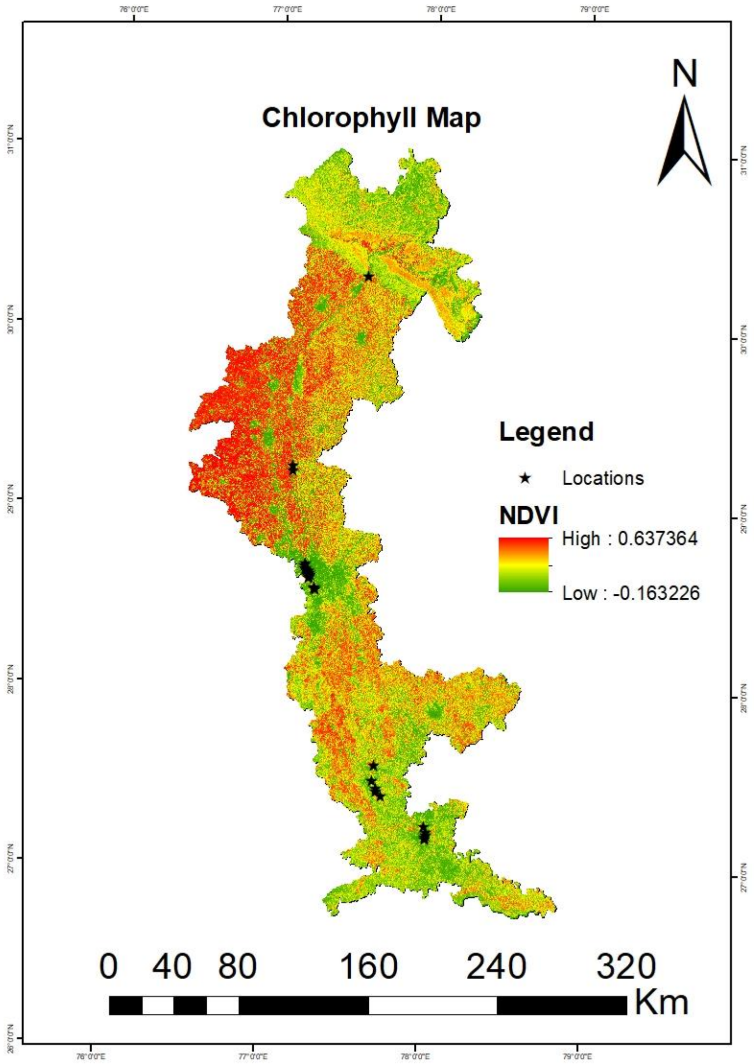

Fig. 4.19: Chlorophyll Map

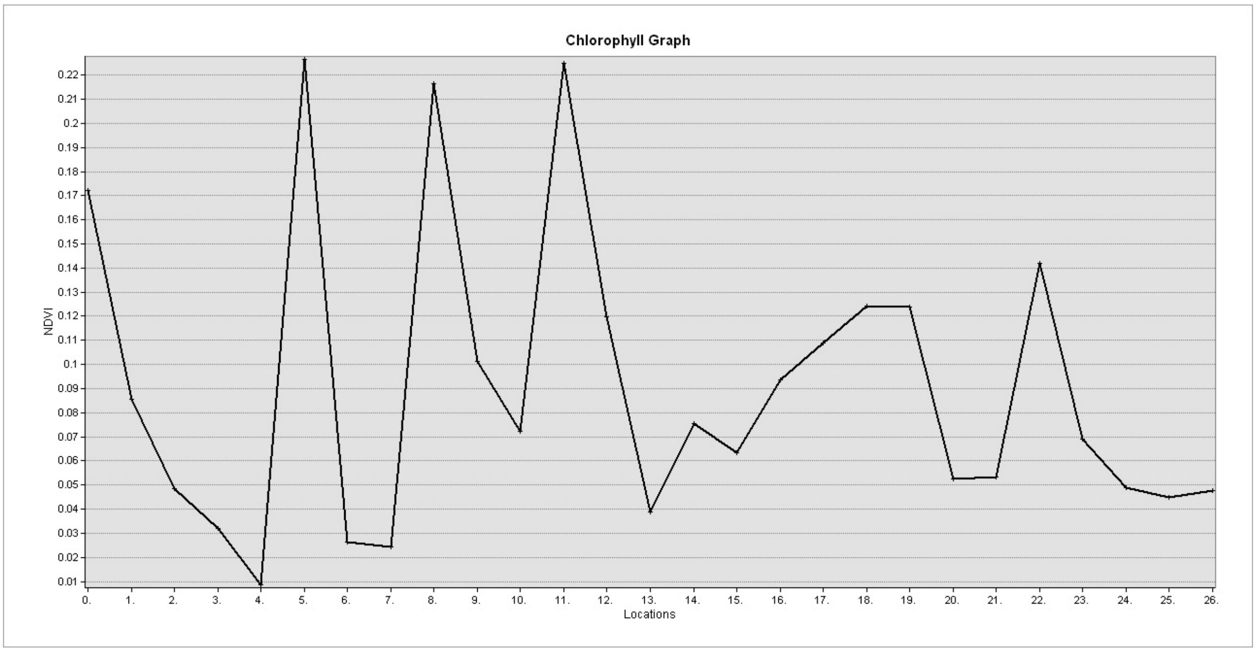

Fig. 4.20: Chlorophyll Graph

F. Total Dissolved Solids

To calculate the total dissolved solids first by using the NDWI we need to located the locations of the water bodies and then apply the algorithm in the model builder to process and get the desired results. There is a range of TDS in mg/L for the reference.

Table 4.8: Range of Total Dissolved Solids

Range (mg/L)	Nearest Recorded
Less than 300	Excellent
300 – 600	Good
600 – 900	Fair
900 – 1200	Poor
Above 1200	Unacceptable

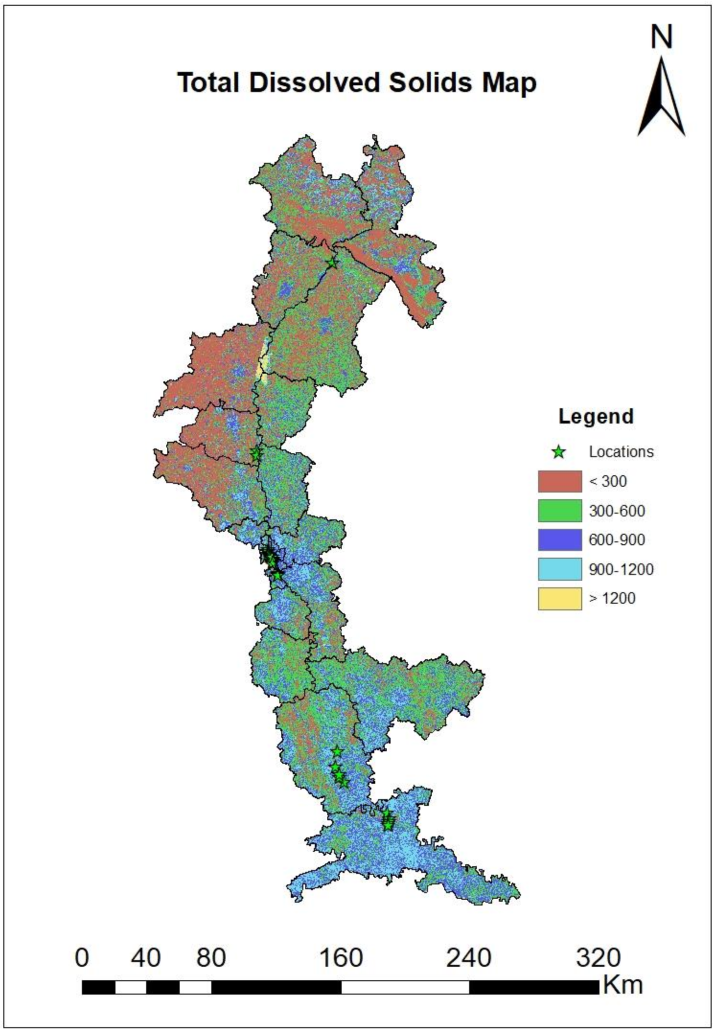

Fig. 4.21: Total Dissolved Solids Map

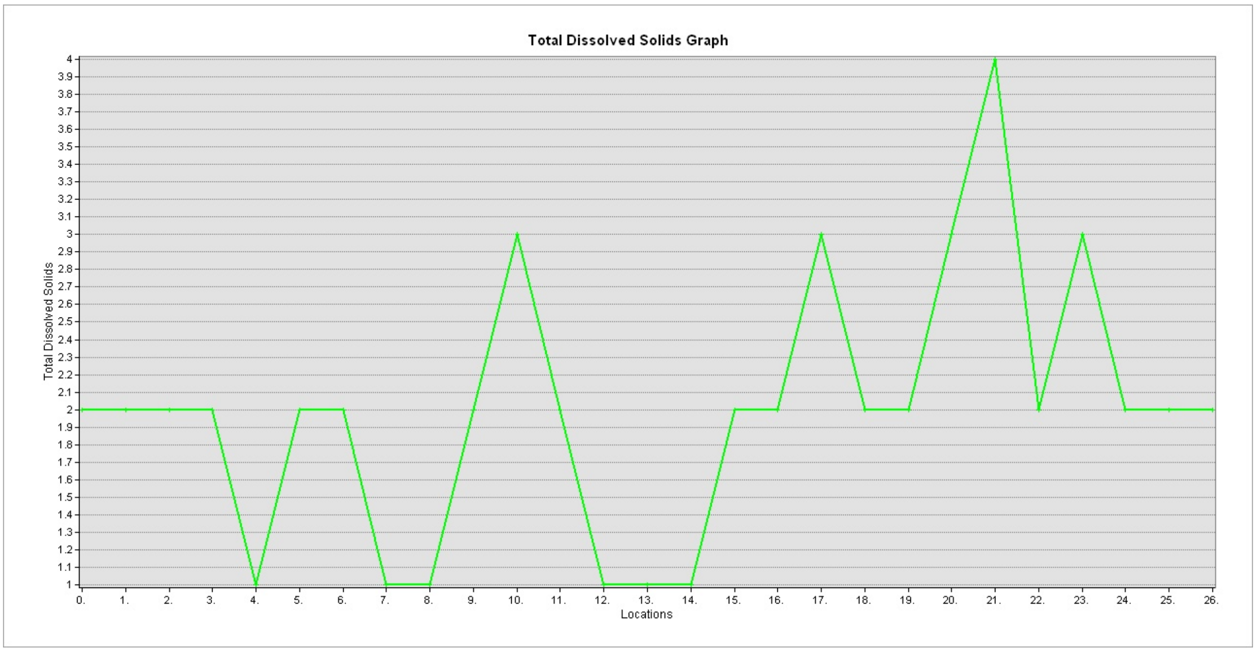

Fig. 4.22: Total Dissolved Solids Graph

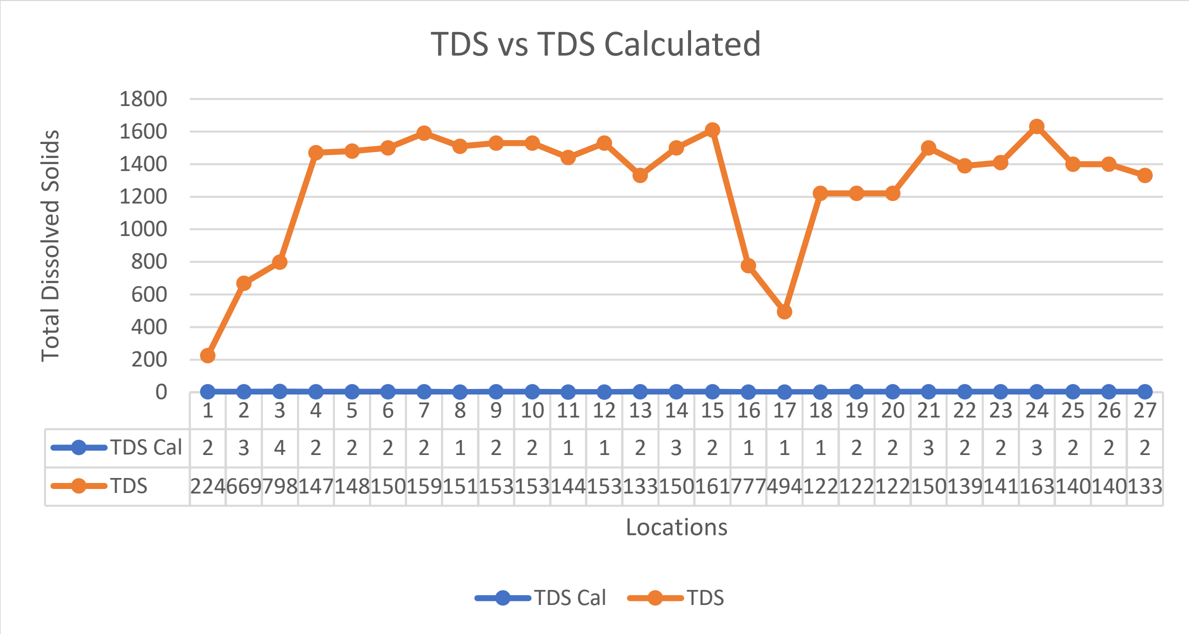

Fig. 4.23: TDS (in-situ) vs TDS (sat)

G. Coloured Dissolved Organic Matter

Coloured dissolved organic matter (CDOM) is the portion of the dissolved organic matter in water that can be seen with the naked eye. The tannins produced by decaying debris are the principal source of CDOM in aquatic environments. Longer-wavelength red light is absorbed by pure water, whereas short-wavelength blue to ultraviolet light is most effectively absorbed by CDOM. With the use of the combination of the Coastal/Aerosol and Blue band which are band 1 and band 2 in Landsat respectively and using the model algorithm equation mentioned below, the results can be generated.

Table 4.9: Range of Coloured Dissolved Organic Matter in mg/L^{-1}

Range (mg/L^{-1})
0 – 10
5 – 50
5 – 70
50 – 200
100 – 500

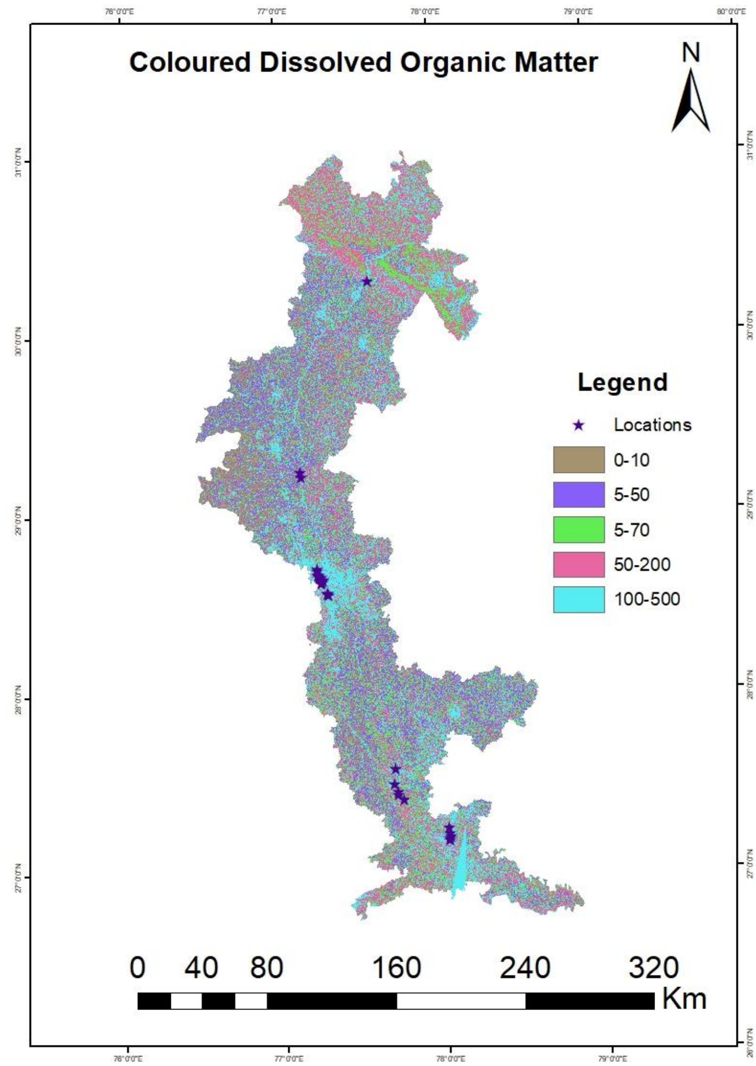

Fig. 4.24: Coloured Dissolved Organic Matter Map

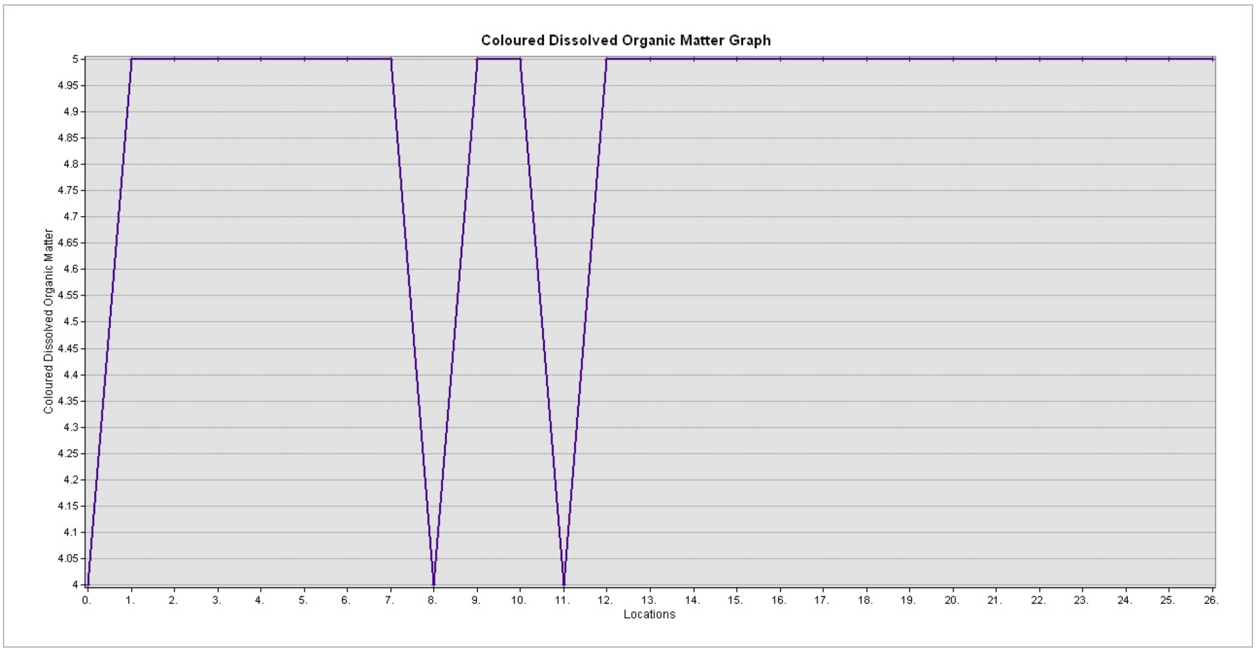

Fig. 4.25: Coloured Dissolved Organic Matter Graph

H. Dissolved Oxygen

The combination of the Blue, Red, Visible and Near Infrared (VNIR) and Short-Wave Infrared (SWIR) bands of 20 m resolution of the sentinel-2 satellite which are Band 2, 4, 6 and 11 respectively are used and the tile-by-tile process is applied by the model algorithm equation mentioned below and then mosaiced and equalized to generate better results for the dissolved oxygen map. The manual reclassification is used to normalize the pixel values accordingly to the universal ranges dissolved oxygen and then the graph is generated and map is exported. For dissolved oxygen the range tends to from 1 to 10 in p.p.m.

Table 4.10: Range of Dissolved Oxygen in p.p.m

Range	Tolerance
< 3	Too low for fish populations
3 – 5	12 – 24-hour range of tolerance/ stressful conditions
6	Supports spawning
> 7	Supports growth/activity
>9	Supports abundant fish populations

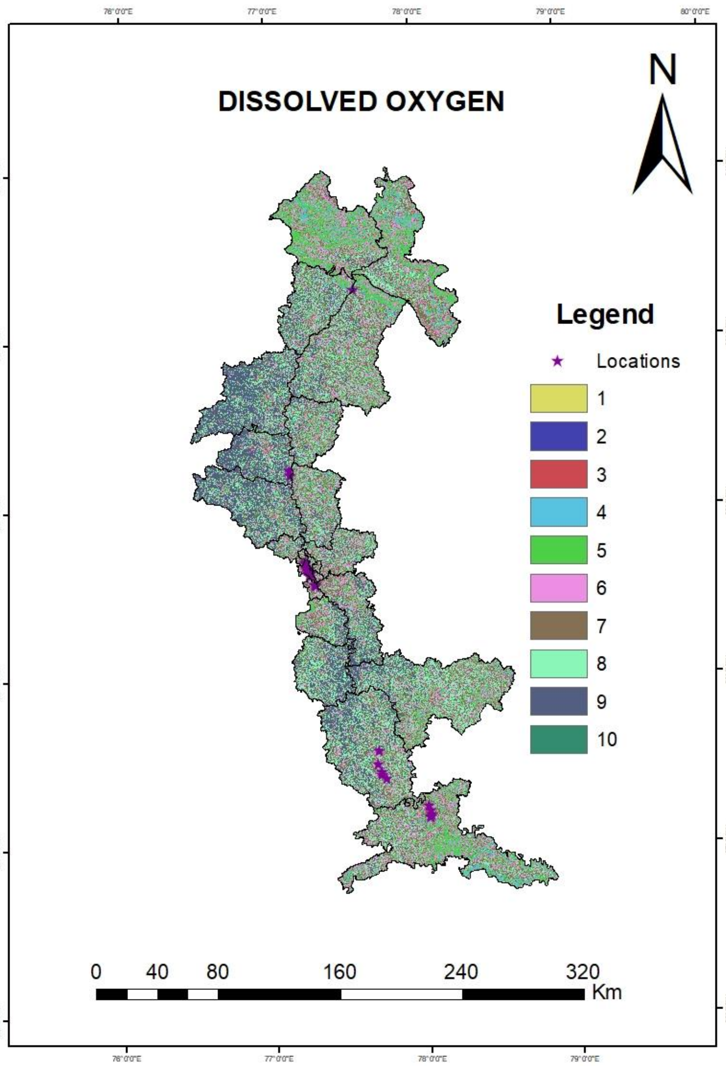

Fig. 4.26: Dissolved Oxygen Map

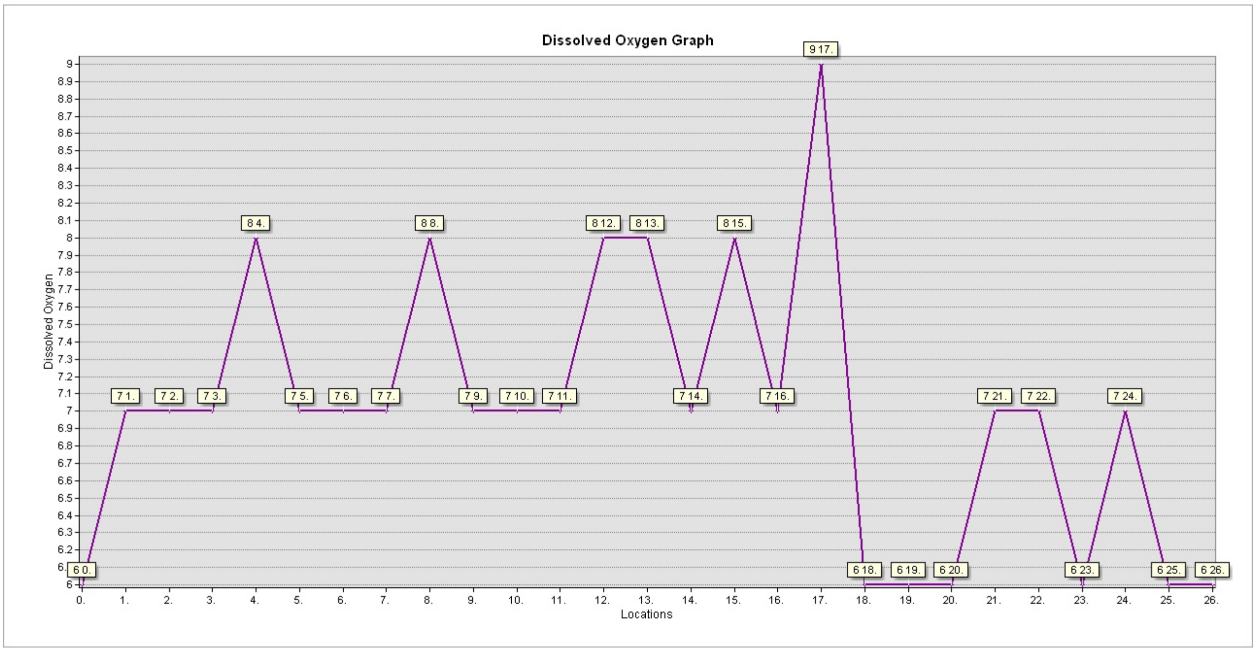

Fig. 4.27: Dissolved Oxygen Graph

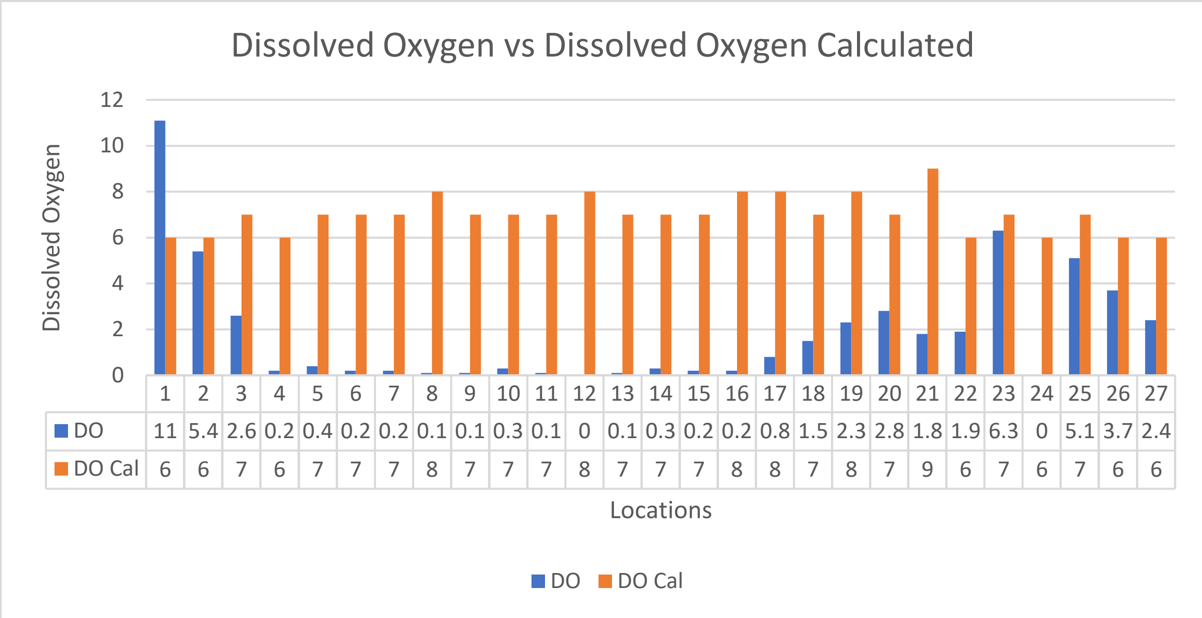

Fig. 4.28: DO (in-situ) vs DO (sat)

4.6 CONCLUSION

The use of remote sensing satellites like the Landsat and Sentinel-2 for the calculation of the water quality is very helpful as they can cover a wide area and routine observation of the water quality using remote sensing can be considered by different organizations as an alternative method to field surveys for recording and processing water quality information for various works. The results obtained help us to better understand how much the river has been polluted and the need to take some measures which can help us in the rejuvenation of the Yamuna River.

The in-situ measurements for validations shows a strong corelation for the pH, TDS, Turbidity and DO. The thermal bands of Landsat satellite also have a strong corelation with the calculated temperature. The other parameters validation can only be done via the visual interpretation classes after the reclassified processing. The reclassified process is manually done to generate the results required according to the spectral library already given.

The spectral band corresponds to a specific characteristic of the water or the substances within it. By analyzing the spectral signatures, it was possible to derive quantitative estimates of water quality parameters. For instance, certain bands can be used to estimate chlorophyll-a concentration, turbidity, or the presence of harmful algal blooms. Compared to traditional field sampling or in-situ measurements, remote sensing can be a more cost-effective method for water quality assessment, especially when considering large-scale monitoring programs. By using satellite data, it is possible to gather information over extensive areas without the need for extensive ground-based monitoring networks. This approach can significantly reduce costs associated with fieldwork and personnel.

[1] A. K. Chaurasia, H. K. Pandey, S. K. Tiwari, R. Prakash, P. Pandey, and A. Ram, "Groundwater quality assessment using water quality index (WQI) in parts of Varanasi District, Uttar Pradesh, India," Journal of the Geological Society of India, vol. 92, pp. 76-82, 2018.

[2] A. K. M. A. Hossain, C. Mathias, and R. Blanton, "Remote Sensing of Turbidity in the Tennessee River Using Landsat 8 Satellite," Remote Sensing, vol. 13, no. 18, p. 3785, Sep. 2021, doi: 10.3390/rs13183785. [Online]. Available: http://dx.doi.org/10.3390/rs13183785.

[3] M. Gholizadeh, A. Melesse, and L. Reddi, "A Comprehensive Review on Water Quality Parameters Estimation Using Remote Sensing Techniques," Sensors, vol. 16, no. 8, p. 1298, Aug. 2016, doi: 10.3390/s16081298. [Online]. Available: http://dx.doi.org/10.3390/s16081298.

[4] M. Wu, W. Zhang, X. Wang, and D. Luo, "Application of MODIS satellite data in monitoring water quality parameters of Chaohu Lake in China," Environmental Monitoring and Assessment, vol. 148, pp. 255-264, 2009.

[5] B. A. Schaeffer, K. G. Schaeffer, D. Keith, R. S. Lunetta, R. Conmy, and R. W. Gould, "Barriers to adopting satellite remote sensing for water quality management," International Journal of Remote Sensing, vol. 34, no. 21, pp. 7534-7544, 2013.

[6] M. J. Alam, M. R. Islam, Z. Muyen, M. Mamun, and S. Islam, "Water quality parameters along rivers," International Journal of Environmental Science & Technology, vol. 4, pp. 159-167, 2007.

[7] O. J. R. Pereira et al., "Estimating Water pH Using Cloud-Based Landsat Images for a New Classification of the Nhecolândia Lakes (Brazilian Pantanal)," Remote Sensing, vol. 12, no. 7, p. 1090, Mar. 2020, doi: 10.3390/rs12071090. [Online]. Available: http://dx.doi.org/10.3390/rs12071090.

[8] X. Wang and W. Yang, "Water quality monitoring and evaluation using remote sensing techniques in China: a systematic review," Ecosystem Health and Sustainability, DOI: 10.1080/20964129.2019.1571443, 2019.

[9] D. Doxaran, R. C. N. Cherukuru, and S. J. Lavender, "Use of reflectance band ratios to estimate suspended and dissolved matter concentrations in estuarine waters," International Journal of Remote Sensing, vol. 26, no. 8, pp. 1763-1769, 2005.

[10] K. P. Sudheer, I. Chaubey, and V. Garg, "Lake water quality assessment from Landsat Thematic Mapper data using neural network: an approach to optimal band combination selection," JAWRA Journal of the American Water Resources Association, vol. 42, no. 6, pp. 1683-1695, 2006.

[11] S. Somvanshi, P. Kunwar, N. B. Singh, and T. S. Kachhwaha, "Water turbidity assessment in part of Gomti River using high-resolution Google Earth’s Quickbird satellite data," in Geospatial World Forum, 2011, pp. 18-21.

[12] S. Somvanshi, P. Kunwar, N. B. Singh, S. P. Shukla, and V. Pathak, "Integrated remote sensing and GIS approach for water quality analysis of Gomti river, Uttar Pradesh," International Journal of Environmental Sciences, vol. 3, no. 1, pp. 62-74, 2012.

[13] "DRINKING WATER — SPECIFICATION (Second Revision)," IS 10500, 2012.

[14] P. K. Meher, P. Sharma, Y. P. Gautam, A. Kumar, and K. P. Mishra, "Evaluation of Water Quality of Ganges River Using Water Quality Index Tool," Environment Asia, vol. 8, no. 1.

[15] J. C. Ritchie, P. V. Zimba, and J. H. Everitt, "Remote sensing techniques to assess water quality," Photogrammetric engineering & remote sensing, vol. 69, no. 6, pp. 695-704, 2003.

[16] Z. Zheng, Y. Li, Y. Guo, Y. Xu, G. Liu, and C. Du, "Landsat-Based Long-Term Monitoring of Total Suspended Matter Concentration Pattern Change in the Wet Season for Dongting Lake, China," Remote Sensing, vol. 7, no. 10, pp. 13975-13999, Oct. 2015, doi: 10.3390/rs71013975.

[17] J. Chen, W. N. Zhu, Y. Q. Tian, and Q. Yu, "Estimation of colored dissolved organic matter from Landsat-8 imagery for complex inland water: case study of Lake Huron," IEEE Transactions on Geoscience and Remote Sensing, vol. 55, no. 4, pp. 2201-2212, Apr. 2017.

[18] E. T. Slonecker, D. K. Jones, and B. A. Pellerin, "The new Landsat 8 potential for remote sensing of colored dissolved organic matter (CDOM)," Marine Pollution Bulletin, vol. 107, no. 2, pp. 518-527, 2016.

[19] D. Katyal, A. Qader, A. H. Ismail, and K. Sarma, "Water quality assessment of Yamuna River in Delhi region using index mapping," Interdisciplinary Environmental Review, vol. 13, no. 2-3, pp. 170-186, 2012.

[20] K. W. Abdelmalik, "Role of statistical remote sensing for Inland water quality parameters prediction," The Egyptian Journal of Remote Sensing and Space Science, vol. 21, no. 2, pp. 193-200, 2018.

[21] A. El-Zeiny and S. El-Kafrawy, "Assessment of water pollution induced by human activities in Burullus Lake using Landsat 8 operational land imager and GIS," The Egyptian Journal of Remote Sensing and Space Science, vol. 20, pp. S49-S56, 2017.

[22] V. Markogianni, D. Kalivas, G. Petropoulos, and E. Dimitriou, "An Appraisal of the Potential of Landsat 8 in Estimating Chlorophyll-a, Ammonium Concentrations and Other Water Quality Indicators," Remote Sensing, vol. 10, no. 7, p. 1018, Jun. 2018, doi: 10.3390/rs10071018.

[23] I. Aslanov, S. Kholdorov, S. Ochilov, A. Jumanov, Z. Jabbarov, I. Jumaniyazov, and N. Namozov, "Evaluation of soil salinity level through using Landsat-8 OLI in Central Fergana valley, Uzbekistan," in E3S Web of Conferences, vol. 258, p. 03012, EDP Sciences, 2021.

[24] K. Toming, T. Kutser, R. Uiboupin, A. Arikas, K. Vahter, and B. Paavel, "Mapping Water Quality Parameters with Sentinel-3 Ocean and Land Colour Instrument imagery in the Baltic Sea," Remote Sensing, vol. 9, no. 10, p. 1070, Oct. 2017, doi: 10.3390/rs9101070.

[25] W. Pimwiset, K. Tungkananuruk, T. Rungratanaubon, P. Kullavanijaya, and C. V. Sillberg, "Water Turbidity Determination by a Satellite Imagery-Based Mathematical Equation for the Chao Phraya River: 10.32526/ennrj/20/202100237," Environment and Natural Resources Journal, vol. 20, no. 3, pp. 297-309, 2022.

[26] M. Arief, "Development of dissolved oxygen concentration extraction model using Landsat data case study: Ringgung coastal waters," International Journal of Remote Sensing and Earth Sciences (IJReSES), vol. 12, no. 1, pp. 1-12, 2017.

[27] A. KC, A. Chalise, D. Parajuli, N. Dhital, S. Shrestha, and T. Kandel, "Surface water quality assessment using remote sensing, GIS and artificial intelligence," Technical Journal, vol. 1, no. 1, pp. 113-122, 2019.

[28] E. E. Cruz-Montes, M. M. Durango-Banquett, F. M. Torres-Bejarano, G. A. Campo-Daza, and C. Padilla-Mendoza, "Remote sensing application using Landsat 8 images for water quality assessments," in Journal of Physics: Conference Series, vol. 2475, no. 1, p. 012007, IOP Publishing, Apr. 2023.

[29] M. C, Mamathi, Aduri Jogendra, Sridhar Pechetty, and R. Selvakumar, "Monitoring Water Quality Parameters Using Satellite Based Remote Sensing Data," 9, pp. 59-71, 2022.

[30] N. Wagle, T. D. Acharya, and D. H. Lee, "Estimating Chlorophyll-a and Dissolved Oxygen Based on Landsat 8 Bands Using Support Vector Machine and Recursive Partitioning Tree Regressions," in The 6th International Electronic Conference on Sensors and Applications, Nov. 2019, doi: 10.3390/ecsa-6-06573.

[31] V. Garg, S. P. Aggarwal, and P. Chauhan, "Changes in turbidity along Ganga River using Sentinel-2 satellite data during lockdown associated with COVID-19," Geomatics, Natural Hazards and Risk, vol. 11, no. 1, pp. 1175-1195, 2020.

[32] T. Seleem, D. Bafi, M. Karantzia, and I. Parcharidis, "Water Quality Monitoring Using Landsat 8 and Sentinel-2 Satellite Data (2014–2020) in Timsah Lake, Ismailia, Suez Canal Region (Egypt)," Journal of the Indian Society of Remote Sensing, vol. 50, no. 12, pp. 2411-2428, 2022.

[33] F. M. Pizani, P. Maillard, A. F. Ferreira, and C. C. de Amorim, "Estimation of water quality in a reservoir from sentinel-2 msi and landsat-8 oli sensors," ISPRS Annals of the Photogrammetry, Remote Sensing and Spatial Information Sciences, vol. 3, pp. 401-408, 2020.

[34] N. Hussain, M. H. Islam, R. Khanam, and M. Iqbal, "Water Quality in Landsat OLI Images," in International Conference on Engineering Research and Practice, 2017, pp. 19-23.

[35] D. Anandababu, B. M. Purushothaman, and B. S. Suresh, "Estimation of land surface temperature using Landsat 8 data," International Journal of Advance Research, vol. 4, no. 2, pp. 177-186, 2018.

[36] A. A. Shopan, G. T. Islam, A. S. Islam, and M. M. Rahman, "Assessment of Water Quality Parameters in the Ganges Delta Using Remote Sensing Techniques," in International

Conference on Climate Change in Relation to Water and Environment (I3CWE-2015), 2015, pp. 1-7.

[37] J. Ferdous, M. T. U. Rahman, and S. K. Ghosh, "Detection of total dissolved solids from Landsat 8 OLI image in coastal Bangladesh," in The Proceedings of The International Conference on Climate Change, vol. 3, no. 1, 2019, pp. 35-44.